Downloaded from https://www.lyellcollection.org by University of St Andrews Library on Jul 24, 2023

Research article

JGS
Journal of the Geological Society

https://doi.org/10.1144/jgs2023-004 | Vol. 180 | 2023 | jgs2023-004

The Burmese Jade Mines belt: origins of jadeitites, serpentinites, and ophiolitic peridotites and gabbros

M. P. Searle[1,2,3]*, R. M. Palin[1], N. J. Gardiner[4], Kyi Htun[5] and J. Wade[1]

[1] Department of Earth Sciences, Oxford University, South Parks Road, Oxford OX1 3AN, UK
[2] Oxford University Museum of Natural History, Parks Road, Oxford OX1 3PW, UK
[3] Camborne School of Mines, University of Exeter (Cornwall Campus), Penryn, Cornwall TR10 9EZ, UK
[4] School of Earth and Environmental Sciences, University of St Andrews, St Andrews, Fife KY169AL, UK
[5] Consultant Geologist, B201, B14 Ward, Thanthumar Street, Okalapa Township, Yangon, Myanmar
MPS, 0000-0001-6904-6398; RMP, 0000-0002-6959-0462; NJG, 0000-0003-3465-9295; JW, 0000-0002-6998-236X
* Correspondence: mike.searle@earth.ox.ac.uk

Abstract: Ophiolitic peridotites in Myanmar (Burma) occur along three major tectonic zones: the Kaleymyo–Nagaland suture along the Indo-Burman Ranges, the Jade Mines belt and the Tagaung–Mytkyina belt. These belts all show harzburgite–lherzolite–dunite peridotites, but the Hpakan-Taw Maw region (Jade Mines belt) also hosts jadeitites, including pure jadeite, mawsitsit (Cr-rich jadeite) kosmochlore (Cr-rich clinopyroxene) and albitite. Jadeitites with high Na and Al contents require either very unusual Al-rich, Si-poor protoliths or extensive fluid metasomatism, or both. The Hpakan jadeitites formed by Na-, Al- (and Si-) metasomatic alteration of pyroxenite–wehrlite intrusions into harzburgite–dunite from widespread fluid alteration. The fluids could have been derived from a mid-Jurassic intermediate pressure subduction event during ophiolite formation and emplacement. In the Lake Indawgyi area, normal ophiolitic peridotites, including harzburgite and dunite with pyroxenite veins, have not been jadeitized. Gabbros related to the Jade Mines ophiolite gave a U–Pb zircon age of 169.71 ± 1.3 Ma (MSWD 2.2), a similar timing to the Myitkyina ophiolite (173 Ma) to the east, suggesting that the ophiolite belts were originally continuous. The jade 'boulders' in the Uru conglomerate beds at Hpakan have also resulted from normal *in situ* serpentinization weathering processes, followed by limited fluvial mass transport processes along the Uru River.

Supplementary material: U–Pb zircon data are available at https://doi.org/10.6084/m9.figshare.c.6655269

Received 4 January 2023; **revised** 27 March 2023; **accepted** 18 May 2023

The Hpakan–Taw Maw region of Kachin state, Myanmar (Burma) contains the world's richest deposits of jade (Figs 1 and 2). The term 'jade' encompasses a wide variety of types, including pure jadeitic pyroxene ($NaAlSi_2O_6$), Cr-rich pyroxene, kosmochlore (ureyite; $NaCrSi_2O_6$), Fe-rich hedenbergite ($CaFe^{2+}Si_2O_6$) and aegirine ($NaFe^{3+}Si_2O_6$)-bearing jadeitites. The highest quality 'imperial jade' is composed of green–black kosmochlore enriched in Cr^{3+} (Gübelin 1965). The mawsitsit variety shows mottled intergrowths of white albite, yellow Mg-chlorite (clinochlore), green–black kosmochlore and chromian jadeite. Other varieties include lavender coloured jade enriched in Fe^{2+}, pale mauve varieties enriched in Mn^{2+} and blue–green varieties enriched in Fe^{2+} and Fe^{3+}. Although jadeite is usually inferred to form at high pressures in subduction zone settings (Sorensen and Harlow 1999; Harlow and Sorensen 2001; Shi *et al.* 2012, 2014), the timing of high-pressure assemblages is often not concomitant, raising some doubt as to the connection (Tsujimori and Harlow 2012). Jadeite can also form by the subsolidus reaction of albite + nepheline → jadeite at low temperatures (250–300°C) and pressures (*c.* 3–5 kbar). The jadeitites in Hpakan are associated with widespread regional serpentinization and CO_2 fluid-fluxing, resulting in a variety of minerals and rock types, including lizardite, chrysotile or antigorite serpentinite, albitite, carbonate- or silica-saturated listwanite (talc + magnesite + silica), opal and chalcedony.

The Jade Mines belt is restricted to an area along the northern part of the Sagaing Fault around Taw Maw and the Uru river valley (Fig. 1). Three main regions have been delineated: the Taw Maw region, where serpentinized peridotites host dykes and veins of jadeite and albitite in outcrop (Noetling 1893; Bauer 1895; Bleeck 1908; Chhibber 1934*a*, *b*; Bender 1983; Hughes *et al.* 2000; Nyunt 2009); a region along the Uru River boulder conglomerates, west of Hpakant (Fig. 3); and a third region around Khampti and the Nansibon jade mine to the west (Fig. 2). Serpentinized peridotites continue southwards to the Lake Indawgyi area, where they do not contain jadeitite dykes. Another belt of serpentinite without jadeite has been mapped to the NW along the western boundary of the Hukawng valley, where Cretaceous–Cenozoic sedimentary rocks affected by folding are unconformably overlain by sub-horizontal Late Miocene and younger sediments of the Irrawaddy Group (Mitchell 2018; Ridd *et al.* 2019).

The origin of the Hpakant jadeitites has long remained a mystery, partly because of their remote location in northern Kachin state, together with political instabilities, the forceful takeover of jade mines by Burmese generals and the Tatmadaw Burmese army, rebel insurgencies (from the Kachin Independence Army) and illegal mining practices resulting in environmental destruction on a grand scale (Global Witness Report 2015). For all these reasons, the Jade Mines have been off-limits and restricted to foreigners for almost as long as they have been known. Most of the jade mined from Hpakant is exported by road to China. The Global Witness Report (2015) estimated the total value of Myanmar jade production as $122.8 billion from 2005 to 2014, most of which is owned by state-owned companies (Myanmar Economic Holdings) and associated Chinese companies. Some boulders and samples can be found in the Mandalay jade market, but the best samples are auctioned at trade fairs in Nay-pi-daw and Bangkok. Only a few Burmese geologists, and even fewer western geologists, have actually been to Hpakant. Our field studies (MS, NG, KH) are based in the Lake Indawgyi region (Kachin state), the Indo-Burma Ranges and the Chin Hills, the Sagaing Fault, the Mogok metamorphic belt, the Tagaung–Myitkyina ophiolite belt, and throughout the northern

© 2023 The Author(s). This is an Open Access article distributed under the terms of the Creative Commons Attribution 4.0 License (http://creativecommons.org/licenses/by/4.0/). Published by The Geological Society of London. Publishing disclaimer: www.geolsoc.org.uk/pub_ethics

Downloaded from https://www.lyellcollection.org by University of St Andrews Library on Jul 24, 2023

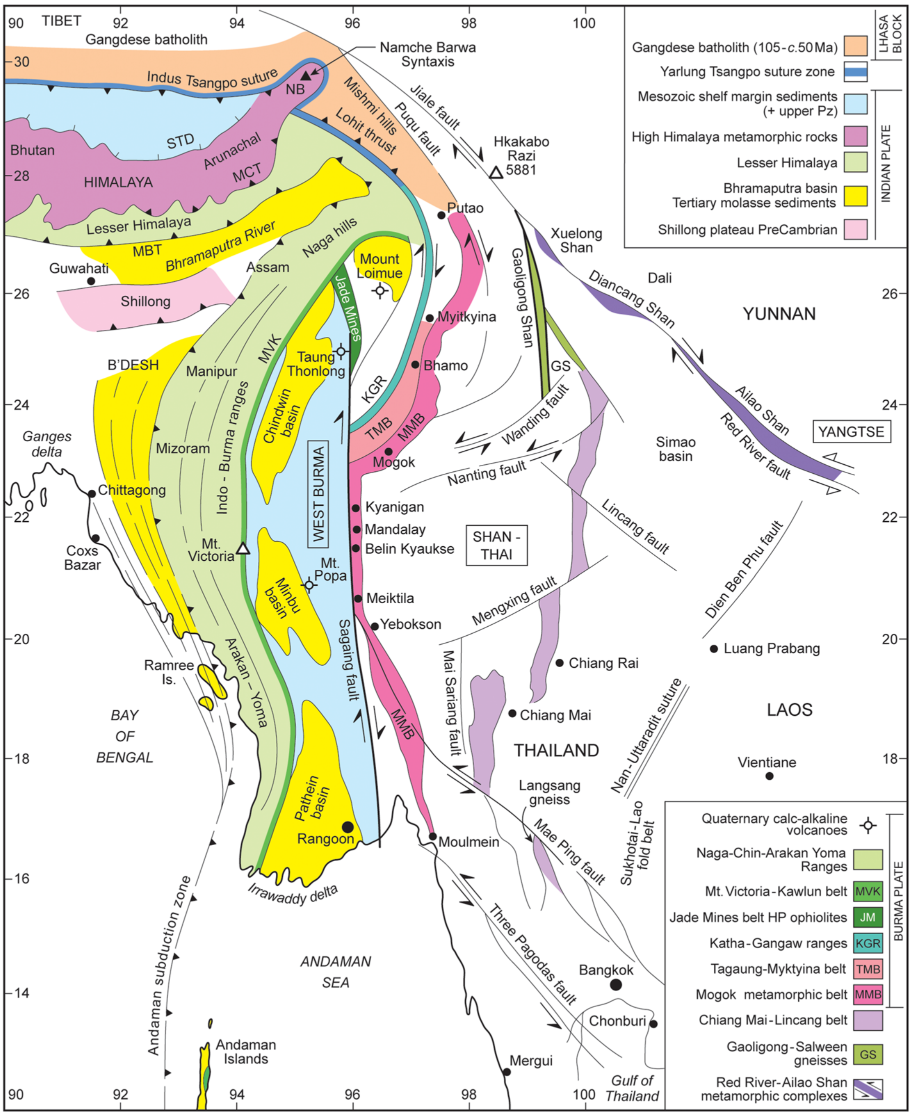

Fig. 1. Structural map of northern Burma (Myanmar) showing the major faults and the location of the Jade Mines belt. Source: Searle *et al.* (2007, 2017) and Myanmar Geosciences Society (2012).

(Putao) and eastern parts of Myanmar. One of us (KH) visited the Hpakant region in 2014.

This paper reviews the occurrence of Burmese jadeitites, and other ophiolitic mantle peridotites, and discusses models to explain their origin. The major questions to be resolved are: are the jadeitites metamorphosed ophiolitic mantle or are they intrusions; is the gabbro from Lake Indawygi related to the Jade Mines peridotites; are the jadeitites related to subduction zone metamorphism; and were the jadeitites of the Jade Mines belt originally part of the Tagaung–Myitkyina belt?

We compare the proposed protoliths of the Burmese jadeitites with similar, but unjadeititized, rocks from the Oman ophiolite mantle sequence and from the Jijal Complex, a sequence of ultramafic rocks (Sapat Complex) and garnet granulites (Jijal Complex) exposed along the base of the Cretaceous Kohistan island arc in the Pakistan Himalaya. We discuss the possible origins of the Hpakant jadeitites and their relationship with the mid-Jurassic to mid-Cretaceous subduction zone responsible for the obduction of ophiolites, and their relationships with the adjacent Pliocene–Pleistocene calc-alkaline volcanoes and the crustal-scale Sagaing dextral strike-slip fault. We conclude that all the ‘jade’ from Hpakant results from the metasomatic alteration of the original supra-subduction zone, ophiolite-related pyroxenites, wehrlites, harzburgites and dunites via the fluxing of Na-, Al- (and Si)-bearing fluids, most of which resulted in serpentinites, although some resulted in pure jadeitite or omphacitite.

Formation of jadeitites

Jadeitites are uncommon rocks made up almost entirely of jadeite pyroxene ($NaAlSi_2O_6$). Jadeitites are thought to form under high-pressure (*c.* 7–20 kbar) and low-temperature (*c.* 300–500°C) metamorphic conditions (Shi *et al.* 2012; Harlow *et al.* 2015) via the alteration of mantle rocks by supercritical fluids enriched in Na, Al and Si, possibly driven off subduction zones (Manning 2004; Stern *et al.* 2013). Tsujimori and Harlow (2012) defined two types of jadeitites: P-type jadeitites crystallizing directly from a hydrous fluid as vein fillings or overgrowths; and R-type jadeitites, a metasomatic replacement of an original sedimentary (e.g. greywacke) or igneous (e.g. albite + quartz) rock. Many jadeitites have vein-like textures, suggesting a metasomatic origin associated with injected fluids. In many localities (e.g. California and Guatemala), jadeitites are associated with high-pressure glaucophane-bearing blueschists and ophiolite-related serpentinites and are commonly related to subduction zone settings (Harlow and Sorensen 2005; Harlow *et al.* 2015).

The high Na and Al contents of jadeitites require either very unusual Al-rich, Si-poor protoliths or extensive metasomatic alteration by fluids, or both. Jadeitites record the transport of large ion lithophile elements (Li, Ba, Sr and Pb), but also more refractory, crustal-derived elements, such as U, Th, Zr and Hf (Ng *et al.* 2016). Common rock-forming replacement minerals include albitite, white mica, omphacite and silica serpentinites. Albitites can form at lower

Downloaded from https://www.lyellcollection.org by University of St Andrews Library on Jul 24, 2023

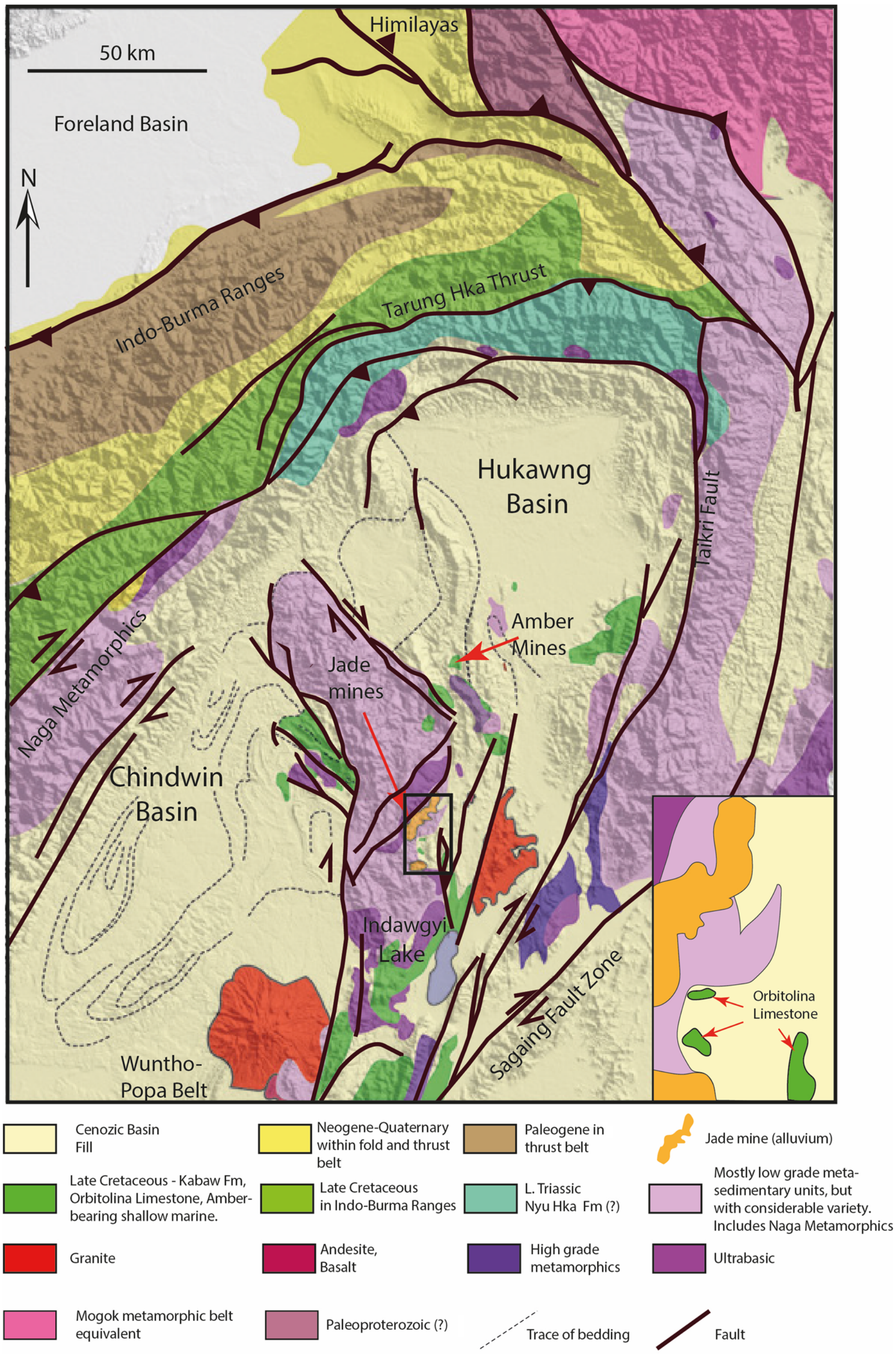

Fig. 2. Geological map of the Jade Mines belt and surrounding region. Source: after Morley *et al.* (2021).

pressures of *c.* 3–8 kbar (Harlow 1994; Okay 1997) and the serpentinization alteration process can occur across a low-temperature spectrum from *c.* 350–300°C to near-surface temperatures. Nephrite jade is usually a product of amphibole (tremolite–actinolite) alteration and is unrelated to high-pressure–low-temperature metamorphic conditions, but related to serpentinization or contact metamorphism between dolomite and an intrusive granite (Stern *et al.* 2013).

Very few of the Burmese 'jade' boulders show an original mantle mineralogy, with most recording extensive fluid alteration, metasomatism and serpentinization on a regional scale. A few Burmese samples from Hpakant show relict orthopyroxene (enstatite) within a serpentinized olivine matrix, suggesting mantle harzburgite as a likely precursor lithology. After the first descriptions by Noetling (1893), Bauer (1895) and Bleeck (1908), jade was thought to occur as intrusive dykes or pods within serpentinite. Since both are the result of regional wholesale metasomatism, this implies that the dykes were probably composed of some sort of pyroxenite intruding an olivine-rich dunite or harzburgite. Similar relatively unaltered examples of these field relationships are seen in the mantle sequence peridotites of the Oman ophiolite and also in the Jijal Complex, in the roots of the Kohistan island arc in the Pakistan Himalaya.

Serpentinization of ophiolite peridotites

Mantle peridotites from ophiolite complexes, including dunite (olivine), harzburgite (olivine + orthopyroxene) and lherzolite (olivine + orthopyroxene + clinopyroxene) are not in equilibrium with surface waters and react with aqueous fluids to form serpentinites. Serpentinization is the process of hydration and alteration of peridotite at low temperatures and is associated with CO_2-rich fluids. Serpentinization is an exothermic reaction that can increase temperatures by up to 300°C and results in an increase in

Downloaded from https://www.lyellcollection.org by University of St Andrews Library on Jul 24, 2023

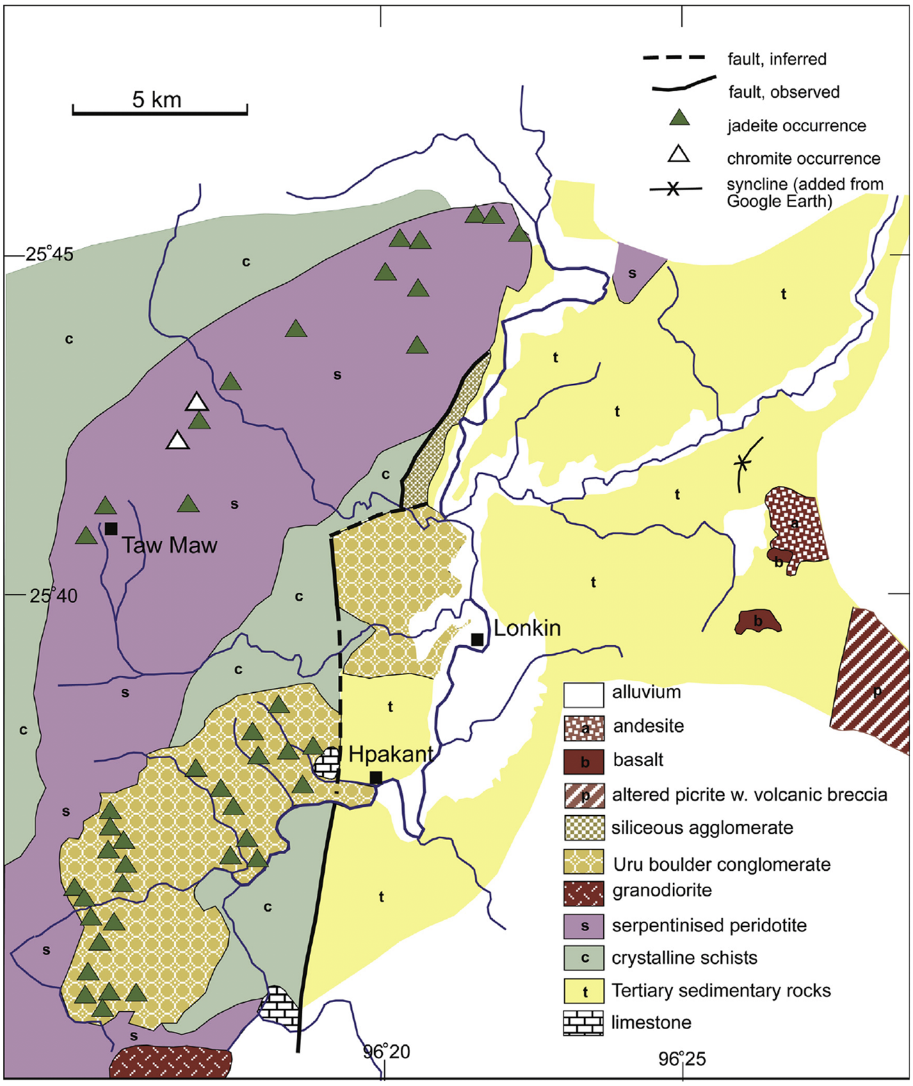

Fig. 3. Geological map of the Taw Maw and Hpakan regions of the Jade Mines belt. Source: after Chhibber (1934*a*, *b*), Bender (1983) and Ridd *et al.* (2019).

volume (Moody 1976). Serpentinites therefore become easily mobile, intruding along fractures, lubricating faults and breaking up country rocks into tectonic mélanges.

In normal harzburgite, the olivine alters to serpentine (chrysotile, lizardite or antigorite) and the orthopyroxene (enstatite) becomes pseudomorphed to bastite. Olivine breaks down in sequence to (1) antigorite + magnesite, (2) magnesite + talc and (3) magnesite + quartz. Olivine and talc do not occur together and neither do serpentine and quartz, showing that each reaction is a progression (Hansen *et al.* 2005). Quartz–carbonate (listwanite) veins can contain Cr-muscovite (fuchsite), opal or chalcedony, and important sulfide–arsenide, Au and Hg mineralization, such as in California and New England (Buckman and Ashley 2010). Pt, Pd and Au are concentrated in Ni–Fe sulfides, along with chromite, which survives all these alteration reactions. Magnetite, however, is consumed during the reaction serpentine/brucite + magnetite + CO_2 → talc + magnesite (Hansen *et al.* 2005). The final products are minerals such as dolomite, brucite and goethite. Most of these reactions lock up CO_2 in magnesite, a process that has the potential for capturing and storing CO_2 in rocks (Kelemen and Matter 2008).

Burmese ophiolite belts

Three main ophiolite belts are recognized in Myanmar (Fig. 1; Hutchison 1975; Mitchell 1993; Searle and Morley 2011; Gardiner *et al.* 2016, 2018; Searle *et al.* 2017). The Western ophiolite belt runs along the Indo-Burma Ranges from the Andaman Sea north to the Hukawng basin and includes the four main ophiolites outcropping in the Chin hills, Myanmar (the Kwekha, Webula, Kaleymo and Yazagyo dam ophiolite blocks) (Morley and Searle 2017; Morley *et al.* 2020) and the Nagaland ophiolites in India (Acharyya 2007, 2010; Ao and Bhowmik 2014). Liu *et al.* (2016) determined a Mid-Cretaceous U–Pb zircon age of *c.* 127 Ma from the Kaleymyo ophiolite. Singh *et al.* (2016) reported $^{206}Pb/^{238}U$ zircon ages of 116.4 ± 2.2 Ma and 118.8 ± 1.2 Ma from the Nagaland–Manipur ophiolite just across the border in eastern India. The Eastern ophiolite belt runs from the Sagaing Fault NE along the Tagaung–Myitkyina belt (Fig. 1) and contains relict ophiolites of likely Middle Jurassic age (Xu *et al.* 2017; Chen *et al.* 2018). Liu *et al.* (2016) determined a U–Pb zircon age of *c.* 173 Ma for the Myitkyina ophiolite. The Central ophiolite belt is composed of the Jade Mines belt, which extends along the northern termination of the western branch of the Sagaing Fault south of the Hukawng basin and does not correspond easily to either the Western or Eastern ophiolite belts (Ridd *et al.* 2019). One suggestion has been that all three ophiolite belts were originally part of the same suture zone, disrupted and offset by strike-slip faults along the Sagaing Fault (Maung 1987; Mitchell 1993; Mitchell *et al.* 2021) giving a total right-lateral offset of >400–450 km.

The Sagaing Fault is a crustal-scale dextral strike-slip fault that runs from the Andaman Sea spreading centre in the south to the Hukawng basin in the north, where it splays into several branches east of the Jade Mines belt (Fig. 1). It is extremely active seismically and accommodates right-lateral strike-slip motion up to 18–22 mm a^{-1} (Vigny *et al.* 2003; Maurin *et al.* 2010; Sloan

Downloaded from https://www.lyellcollection.org by University of St Andrews Library on Jul 24, 2023

et al. 2017). The fault abruptly cuts granulite facies gneisses, migmatites and syenites of the Mogok Metamorphic belt to the east. Mogok metamorphism has been precisely dated by U–Pb monazite, titanite and zircon techniques to 43–32 Ma, with a later upper amphibolite sillimanite grade event peaking at 23–20 Ma (Searle *et al.* 2007, 2020; Lamont *et al.* 2021), constraining the oldest age of shearing along the Sagaing Fault. Along the western margin of the Sagaing Fault the North Minwun basin is a synkinematic basin formed along a releasing bend. Detrital zircons and titanites have given maximum depositional ages of 28–27 Ma, providing an older time constraint on the initiation of right-lateral shearing (Morley and Arboit 2019). Using the initiation ages and offsets along the Sagaing Fault, a reconstruction shows that a *c.* 400 km dextral offset is feasible and that the simplest explanation for the geology is that the ophiolite belt along the Nagaland–Kaleymyo part of the Indo-Burman Ranges was originally contiguous with the ophiolite along the Tagaung–Myitkyina belt.

Normal peridotite mantle sequence rocks (harzburgites and dunites) occur along every ophiolite belt in Myanmar and SE Asia; however, only the Jade Mines belt around Taw Maw and Hpakant contains jadeitites, omphacitites and other high-pressure peridotites. A third area of jadeite mining is the Khamti region on the upper Chindwin river NW of the Chindwin basin, although field relationships here are very poorly known.

Jade Mines belt, Myanmar

The first geological descriptions of the Jade belt were made by Noetling (1893), Bauer (1895) and Bleeck (1908), who described veins of jadeite with a white albite rim intruding serpentinites. The main jadeite outcrops and mines are shown on the original maps of Chhibber (1934*a*, *b*), maps that have been redrawn in many subsequent papers. Chhibber's map (Fig. 3) shows a dominant north–south belt of serpentinized peridotite outcrops around Taw Maw and a belt of young Pliocene–Pleistocene boulder conglomerates along the Uru River (Fig. 4). Although some outcrops are present, most mining is carried out by large-scale, environmentally disastrous strip mining, resulting in numerous landslides (Hughes *et al.* 2000). There are some descriptions of amphibolites, actinolite schists, garnet–mica schists and glaucophane–epidote schists in the Jade Mines area (Chhibber 1934*a*, *b*; Nyunt 2009; Nyunt *et al.* 2017). Nyunt (2009) described glaucophane, phengite and epidote schists intercalated with garnet–mica schist associated with jadeitites. Most outcrops and boulders in the Hpakant and Taw Maw areas show a variety of serpentinized peridotites and jadeitites. Jadeitites have variable mineral assemblages, including jadeite ± kosmochlore ± omphacite ± albite ± amphiboles. Albite + jadeite rocks are thought to be metamorphosed plagiogranite-type igneous rocks, intruded into the peridotite (Coleman and Wang 1995). Cr-rich jadeite almost certainly has an origin related to the chromite-bearing peridotites of the mantle sequence.

Jadeitite outcrops around Taw Maw

The main outcrops of jadeitites occur along a north–south belt centred around Taw Maw (Fig. 3; Chhibber 1934*a*, *b*; Nyunt 2009). Massive cliffs of green jadeitite (Fig. 4a) are intruded by white veins and dykes of albitite (Fig. 4b). Bleeck (1908) also describes jadeitite dykes with rims of albitite and amphibolite intruding serpentinite (Harlow *et al.* 2015). The albitites have been interpreted as the metasomatic alteration of an igneous albite granite intrusion, possibly a trondhjemite or plagiogranite, similar to the jadeitites reported from the Monviso ophiolite in the western Alps (Compagnoni *et al.* 2012). The Taw Maw outcrop photographs clearly show massive outcrops of green jadeitites that have been extensively mined, resulting in huge landslides (Fig. 4c, d). Jadeitite can be dark green, white or purple depending on the minor accessory elements. Also described from Taw Maw are black omphacitites, green kosmochlor-bearing peridotites, jadeite amphibolite, albitites and jadeitized rodingite (Shi *et al.* 2012). Bleeck (1908), Harlow and Sorensen (2005) and Harlow *et al.* (2015) described contact relationships along a jadeitite dyke intruding serpentinite from Taw Maw with albitite progressing outwards from the jadeitite core zone to eckermannite–glaucophane amphibolite.

The most widespread jadeitite shows a heterogeneous metasomatic texture, often with stringers of black omphacitite (Fig. 5a). Some jadeitites have the distinctive green Cr-rich pyroxene kosmochlore (ureyite; $NaCrSi_2O_6$), white albitite and stringers of black omphacitite (Fig. 5b). Some boulders of jadeitite from Hpakant show relict peridotite textures with green clinopyroxene and pale olivine altered to serpentine (Fig. 5c). Less common are the pale purple jadeitites, which show enrichment of Mn and Fe

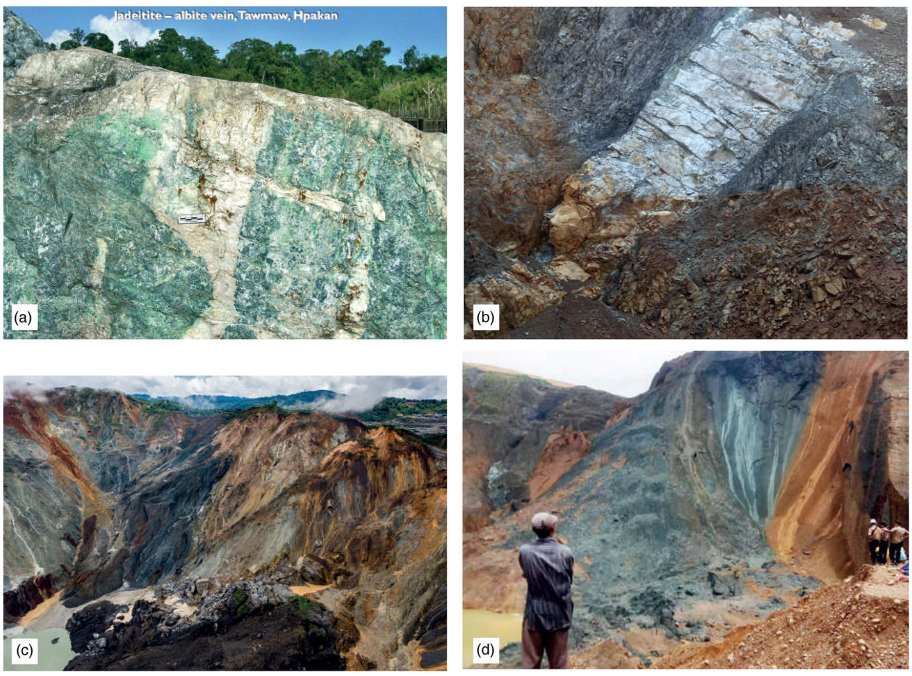

Fig. 4. Field photographs from the Taw Maw area of the Jade Mines belt. (**a**) Outcrop of green jadeitite with an intrusive dyke of white albitite, interpreted as a metasomatized plagiogranite. (**b**) White albitite dyke intruding mantle rocks altered to jadeitite. (**c**) Mountains of bedrock jade around Taw Maw. (**d**) Massive landslip in the jade mines of Taw Maw. Source: parts (a, b), courtesy of Doug Kirwin; parts (c, d) courtesy of *Myanmar Times*.

Downloaded from https://www.lyellcollection.org by University of St Andrews Library on Jul 24, 2023

(Fig. 5d). The most valuable jadeitite is the green ‘imperial jadeitite’, called mawsitsit after the village north of Taw Maw where this rare rock was originally found (Fig. 5e). All rock types show ubiquitous metasomatic textures with white albitite and green jadeitite, sometimes in injected veins (Fig. 5f).

Apart from the world’s best-quality jade, chromite hosted within serpentinized peridotites is also mined from the Taw Maw area. In thin section, blades of kosmochlor-rich pyroxene surround black chromite, with interstitial green jadeite (Searle *et al.* 2017). Jadeite has been overprinted by amphibole–albite assemblages with dark green relict clinopyroxene. In other samples, dark green kosmochlor is enclosed in Cr-omphacite that is partly broken down to a symplectite with albite (Searle *et al.* 2017). Country rocks have been described as glaucophane schists, garnet–mica schists, stilpnomelane quartzites, garnet-bearing amphibolites and diopside-bearing marbles (Chhibber 1934*a*, *b*; Shi *et al.* 2001, 2012; Nyunt 2009; Nyunt *et al.* 2017).

Jadeite boulder beds of the Uru River

Most of the jade from Burma is produced from the Uru River boulder conglomerates, a zone *c.* 15 km long and 5–6 km wide, along which up to 300 m thickness of conglomerate were formed along the banks of the Uru River (Fig. 6a–d). The conglomerates are widely thought be recent Quaternary deposits formed by fluviatile processes transporting boulders downstream. Bender (1983) suggested these could be up to 10 km thick. They are flat-bedded to gently tilted and apparently overlie a metamorphic ‘basement’ composed of various schists, amphibolites and low-grade greenschists (Chhibber 1934*a*, *b*). However, almost all the boulders are serpentinites or jadeitites, with minor garnet-bearing schists and amphibolites, and the matrix is serpentinite. A few boulders in the conglomerates are reported to be red chert, quartzite and gabbro. Some boulders are extremely large, up to 7–10 m in diameter, and all are well rounded. The roundness, however, largely results from the normal weathering of peridotites. Sedimentary structures, such as cross-bedding and channel-fill, are testament to a later fluviatile depositional environment.

During serpentinization, a 3D chessboard structure of veins composed of antigorite, chrysotile, talc, asbestos and clay minerals separates less serpentinized blocks of peridotites within each block. Eventually, the soft-weathering veins are completely mobilized and release now-rounded ‘boulders’ of peridotite, which simply fall out. Similar boulder conglomerates are extremely common along many wadis cutting through peridotites of the Oman ophiolite mantle sequence (Fig. 6f). In the Uru River, it is suggested that many of the boulder conglomerates were formed in this manner, with only minor late-stage fluviatile processes playing a part. The small size of the Uru River and the relatively gentle gradient cannot provide the energy to form these extensive and thick conglomerates by purely fluviatile processes.

Petrology and petrogenesis of the Hpakan jadeitite

Here, we report the results of petrographic observations and electron probe microanalysis performed on a sample of strongly serpentinized peridotite from Hpakant. This sample (JM-7) contains millimetre-scale Al-chromite nodules (0.34–0.36 Al and 1.55–

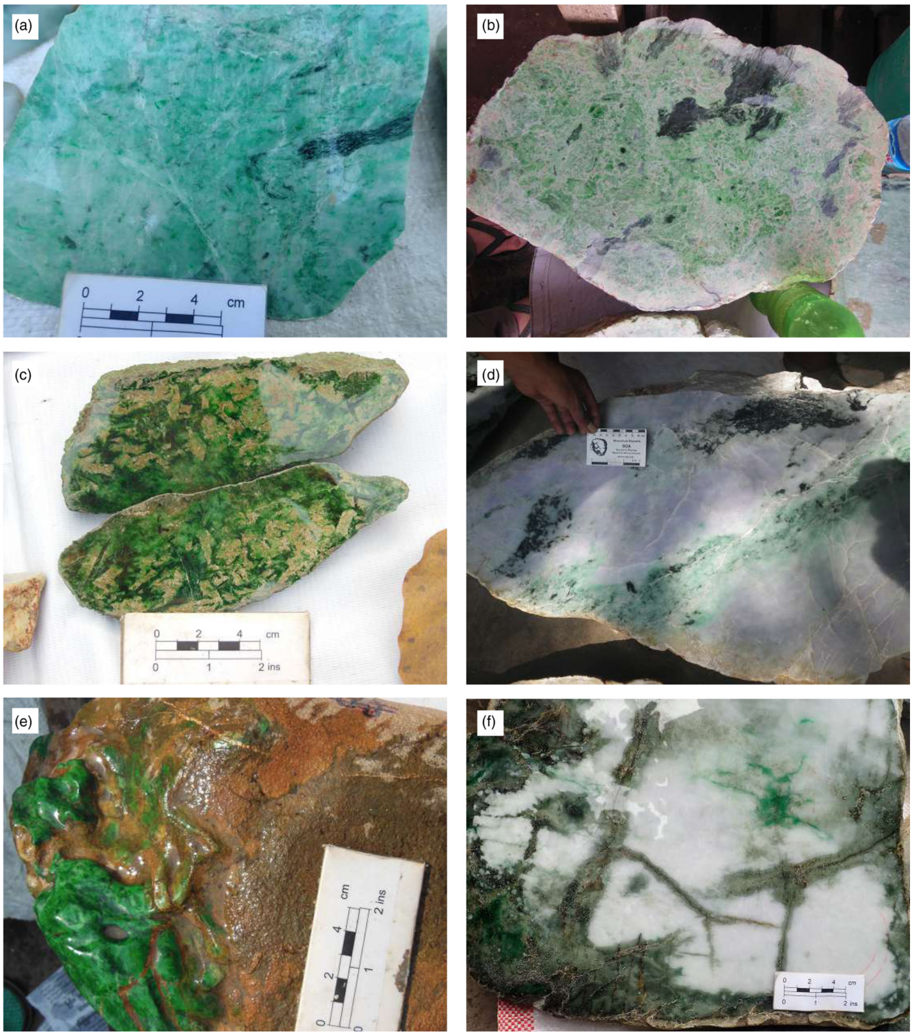

Fig. 5. Varieties of jadeitites from the Taw Maw and Hpakant regions. (**a**) Jadeitite showing metasomatic texture with a stringer of black omphacitite. (**b**) Heterogeneous jadeitite with green kosmochlore, white albitite and stringer of black omphacitite. (**c**) Boulders of jadeitite showing relict peridotite textures with green clinopyroxene and pale olivine altered to serpentine. (**d**) Pale purple jadeitite with stringers of black omphacitite. (**e**) Imperial green jadeitite of variety mawsitsit. (**f**) Albitite and jadeitite in metasomatic contact.

Downloaded from https://www.lyellcollection.org by University of St Andrews Library on Jul 24, 2023

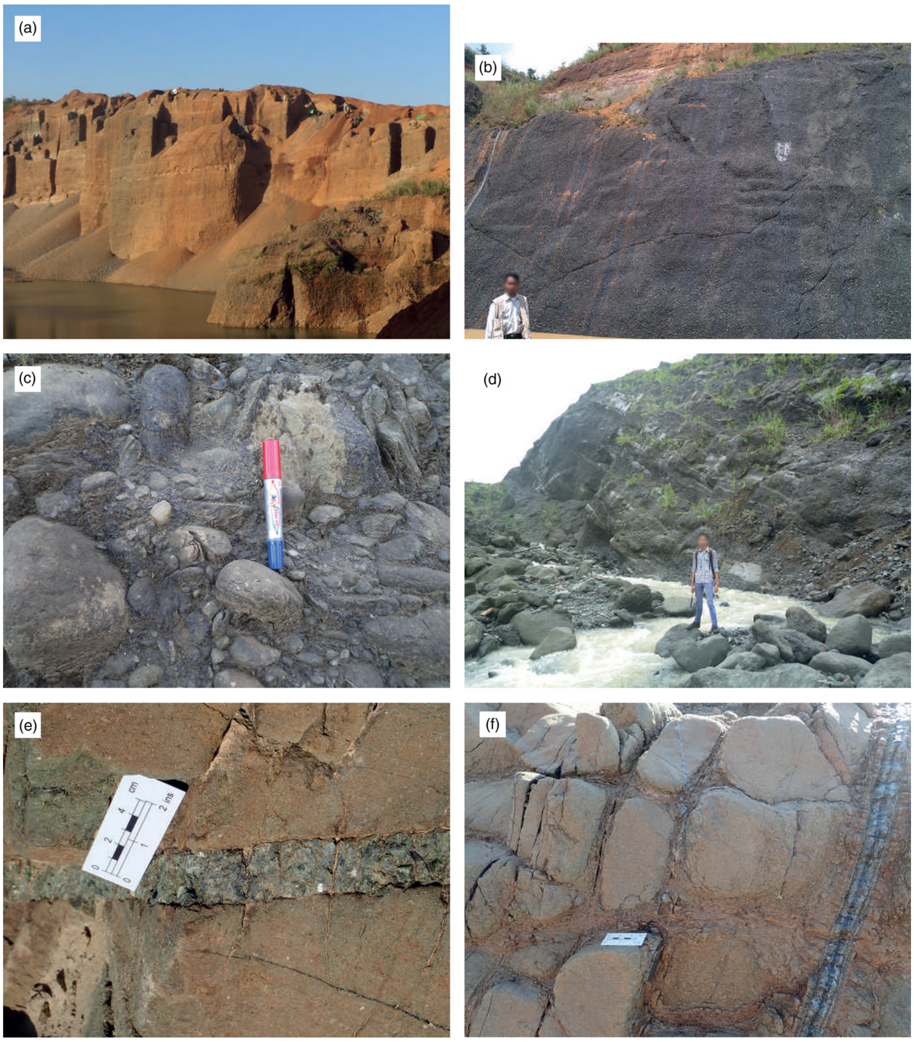

Fig. 6. Field photographs from the Hpakant region of the Jade Mines belt. (**a**) Cliffs *c.* 60 m high of 'bedded' conglomerates consisting almost entirely of boulders of serpentinized peridotites and jadeitites, Uru River. (**b**) Outcrops of boulder conglomerates with clasts of jadeitite and serpentinized peridotites along the Uru River, Hpakant. (**c**) Close-up of the boulder conglomerates showing boulders of serpentinized peridotites in a sheared serpentinite matrix. (**d**) Bedded conglomerates along the Uru River showing gentle tilting of the Uru boulder conglomerates, Hpakant. (**e**) Orthopyroxenite dyke intruding harzburgite mantle sequence, Oman ophiolite. (**f**) Weathering of mantle sequence peridotites showing typical chessboard veining of ultramafic rocks. The veins consist of serpentinite + talc + asbestos. The more solid blocks are normal serpentinized harzburgites and dunites, which weather out and drop to form a loose boulder conglomerate, similar to the Uru boulder beds. A vein of layered orthopyroxenite (enstatite altered to bastite) can be seen on the right; Oman ophiolite mantle sequence.

1.56 Cr for every four oxygen atoms) that are rimmed and partially replaced by Cr-clinopyroxene, which has a typical composition of $Na_{0.92–0.97}Mg_{0.01–0.05}Fe^{2+}_{0.02–0.11}Al_{0.09–0.14}Fe^{3+}_{0.04–0.13}Cr_{0.66–0.84}Si_{1.96–2.00}O_6$ (Table 1) and thus is the variety kosmochlor. The matrix consists of Cr-rich amphibole, mainly of the varieties chromio-nybøite and chromio-eckermannite, and minor serpentine (Table 1). Both the Cr-rich amphibole and serpentine occur as fingers/veins between disaggregated Al-chromite and kosmochlor, which is consistent with them having formed via the metasomatic replacement of the former anhydrous peridotitic assemblage.

Several geological models have been proposed for jadeitite formation. Because all these scenarios require metasomatism, isocon analysis (Grant 2005) was performed to quantify the magnitude of enrichment or depletion of key chemical components between a typical jadeitite and potential protoliths (harzburgite and dunite), with pyrolite also considered for reference (Fig. 7). Here, we considered changes in the $MnO–Na_2O–CaO–K_2O–FeO–MgO–Al_2O_3–SiO_2–TiO_2–O_2$ (MnNCKFMASTO) chemical system. On isocon plots, a central 1:1 dashed line represents no compositional difference (i.e. mass transfer) between the jadeitite and the potential protolith being considered, which would require that a component had the same concentration in both the protolith and the altered product. All the components that lie above the central dashed line represent oxides that are enriched in jadeitite relative to the protolith, and vice versa for the oxides that lie below this line.

Bulk-rock geochemistry could not be obtained for the studied sample (JM7) given its small size. Furthermore, its heterogeneity indicates that a large volume would be required for crushing to produce a homogeneous composition representative of the rock as a whole. As such, we chose to use a jadeitite composition from the Southern Motagua mélange, Guatemala (Harlow *et al.* 2015), which was described as being typical of jadeites worldwide. Previous investigations of jadeitite geochemistry indicate that there are only minor variations between examples worldwide (Tsujimori and Harlow 2012) and therefore, due to the lack of bulk-rock geochemical data for sample SM7, we considered the Southern Motagua mélange here. Data for pyrolite were taken from Ringwood (1975) and data for pristine harzburgite and dunite were taken from Wulff-Pedersen *et al.* (1996).

The calculated isocon (Fig. 7) shows that FeO, MgO and MnO are consistently depleted in jadeitite compared with pyrolite, harzburgite and dunite, with FeO and MnO having lower concentrations by a factor of *c.* 1:10, whereas the MgO content of jadeitite is lower than all proposed protoliths by a factor of *c.* 1:80. All the data for these three oxides are tightly clustered, showing relatively small variance in their protolith concentrations. By contrast, aside from SiO_2, which shows only minor enrichment in the jadeitite (*c.* 1.5:1), the other oxides show considerable scatter in their original protolith concentrations and the degree of enrichment in the jadeitite. For example, CaO is weakly enriched in the jadeitite when compared with a dunite or harzburgite protolith, but is slightly depleted when compared with a harzburgite protolith (Fig. 7). Both TiO_2 and K_2O show moderate enrichment in the jadeitite by ratios up to *c.* 10:1; however, both Al_2O_3 and Na_2O show extreme enrichment in the jadeitite by as little as *c.* 6:1 for Al_2O_3 in pyrolite and up to *c.* 90:1 for Na_2O in harzburgite (Fig. 7).

Downloaded from https://www.lyellcollection.org by University of St Andrews Library on Jul 24, 2023

Table 1. *EPMA-derived mineral compositions from the studied jadeitite. Top rows are reported in wt% oxides and bottom rows are reported in cations per formula unit (cpfu). XMg = molar Mg/(Mg + Fe^{2+}) and XFe^{3+} = Fe^{3+}/Fe^{total}*

Mineral	Al-chromite	Cr-amphibole	Kosmochlor
SiO_2	0.02	54.77	53.40
TiO_2	0.10	0.01	0.06
Al_2O_3	9.07	1.39	2.06
Cr_2O_3	60.09	11.42	26.11
Fe_2O_3	3.28	0.00	2.51
FeO	13.62	2.39	2.50
MnO	0.18	0.03	0.03
MgO	12.66	15.38	0.14
CaO	0.01	0.05	0.02
Na_2O	0.02	10.41	13.18
K_2O	0.01	0.27	0.00
Total	99.06	96.12	100.01
Si	0.00	7.83	2.01
Ti	0.00	0.00	0.00
Al	0.35	0.23	0.09
Cr	1.56	1.29	0.78
Fe^{3+}	0.08	0.00	0.07
Fe^{2+}	0.38	0.29	0.08
Mn	0.01	0.00	0.00
Mg	0.62	3.28	0.01
Ca	0.00	0.01	0.00
Na	0.00	2.89	0.96
K	0.00	0.05	0.00
Sum	3.00	15.87	4.00
Oxygen	4	23	6
XMg	0.62	0.92	0.09
XFe^{3+}	0.19	0.00	0.44

The degree of enrichment and depletion in jadeitite compared with potential ultramafic protoliths is a function of the mobility of different species at crustal or mantle pressures, temperatures and redox conditions. TiO_2 is known to be relatively immobile in metamorphic and metasomatic systems and it is clear that a typical jadeitite is only mildly enriched in TiO_2 compared with dunite and harzburgite, supporting this previous interpretation. However, alkali elements have very high solubilities in aqueous fluids under both crust and mantle conditions, supporting past interpretations that the extreme enrichment in Na_2O suggested by the isocon analysis requires high-volume fluid–rock interactions to convert an Na-poor orthopyroxene or clinopyroxene precursor into an Na-rich jadeititic pyroxene. This supports formation in a geological environment dominated by devolatilization.

To complement the isocon analysis, the stability of jadeitite in convergent margin settings was investigated using phase diagram analysis. Figure 8 shows a *P–T* pseudo-section constructed using Theriak–Domino (De Capitani and Petrakakis 2010) and the internally consistent thermodynamic dataset ds-62 (Holland and Powell 2011) for jadeitite from the Southern Motagua mélange, Guatemala (Harlow *et al.* 2015) under fluid-saturated conditions. Calculations were performed in the Na_2O–CaO–K_2O–FeO–MgO–Al_2O_3–SiO_2–H_2O–O_2 (NCKFMASHO) system using activity–composition (*a–X*) relations from Jennings and Holland (2015), alongside the pure phases talc, lawsonite, kyanite, quartz, rutile, titanite and albite. Uncertainty on the absolute positions of assemblage field boundaries are estimated to be *c.* ±1 kbar and ±50°C at the 2σ level (Palin *et al.* 2016).

Many previous workers have performed conventional thermobarometry on jadeitites from around the world and suggest that recrystallization and equilibration occurs at *c.* 7–21 kbar and *c.* 300–600°C, as shown by the blue field in Figure 8. The calculated *P–T*

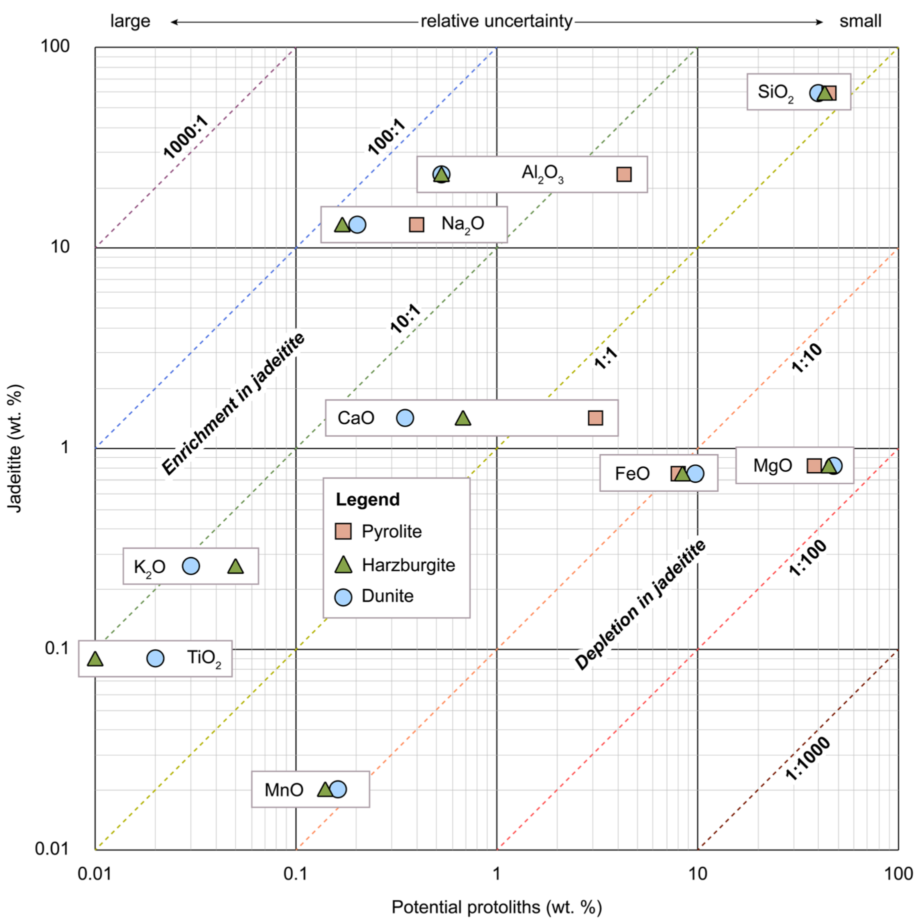

Fig. 7. Isocon showing compositional differences between jadeitite (vertical axis) and proposed protoliths of dunite, harzburgite and pyrolite (horizontal axis). Component oxides that lie below the central 1:1 line are relatively depleted in jadeitite and those that lie above the central 1:1 line are relatively enriched.

Downloaded from https://www.lyellcollection.org by University of St Andrews Library on Jul 24, 2023

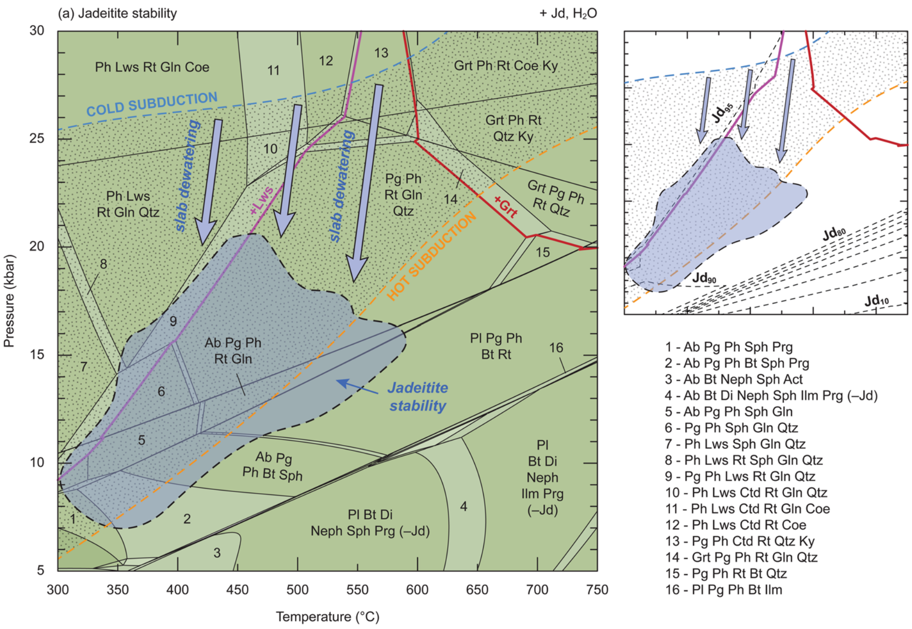

Fig. 8. Pressure–temperature pseudo-section showing the mineral assemblage stability fields for a typical jadeitite composition. Mineral abbreviations after Whitney and Evans (2010). The stippled region represents the range of pressure–temperature conditions on subducting slab surfaces at convergent margins worldwide. Cold and hot subduction zone extremes are marked. Source: Syracuse *et al.* (2010).

pseudo-section additionally shows the stability of other key silicate minerals that may occur within jadeite. For example, garnet would stabilize in jadeitite above 600°C and 20 kbar (Fig. 8, red line) and lawsonite would be stable at low-*T* and high-*P* conditions (Fig. 8, purple line). The stippled region on Figure 8 shows the range of slab-top *P*–*T* profiles recorded by modern day subduction zones (Syracuse *et al.* 2010). It is notable that most *P*–*T* data for jadeitite examples worldwide lie on the low-temperature side of a slab-top thermal profile for a Cascadia-type 'hot' subduction zone, precluding their formation in such environments. By contrast, a Honshu-type 'cold' subduction zone has a slab-top thermal profile that allows the subduction of oceanic crust and associated sediments, heating and metamorphism to drive devolatilization, and the ascent of these fluids through the overlying mantle wedge into the region of *P*–*T* space that most jadeitites record for equilibration (Fig. 8, blue arrows). These results support a model of jadeitite formation in a supra-subduction zone environment where mantle peridotite is strongly metasomatized, with the continuous supply of descending oceanic crust and associated marine sediments providing a readily available source for aqueous fluids to enter the overlying wedge.

U–Pb zircon ages from Burmese jadeitites

A few studies have reported U–Pb ages from zircons in ophiolitic peridotites, but their interpretation remains problematic. Zircon is an extremely uncommon mineral in any mantle rock and, where it does occur, it must have been introduced into the mantle by either metasomatic fluids or as xenocrysts of crustal material recycled into the mantle during subduction (Shi *et al.* 2008; Zhou *et al.* 2014). Robinson *et al.* (2015) identified three groups of zircon ages from Myanmar jadeitite, which they interpreted as follows: Group 1 zircons (mean age 163.2 ± 3.3 Ma) indicating an igneous or hydrothermal event in the Middle Jurassic; Group 2 zircons (mean age 146.5 ± 3.4 Ma) containing jadeitic pyroxene inclusions, suggesting the timing of high-pressure formation; and Group 3 zircons (mean age 122.2 ± 4.8 Ma) representing a later unknown thermal event. Yui *et al.* (2013) also published U–Pb zircon ages from Myanmar jadeitite and obtained ages of 160 ± 1 Ma, which they interpreted as an igneous protolith age, and 77 ± 3 Ma, which they interpreted as the age of formation of jadeitite. Yui *et al.* (2013) proposed that the older Jurassic ages obtained by Shi *et al.* (2008) resulted from incompletely inherited zircon and that their Late Cretaceous age recorded the subduction event.

Given that the Hpakan jadeitites likely formed via wholesale metasomatic replacement, it is difficult to place any meaningful geological interpretation on these zircon ages. Fu *et al.* (2010) concluded that $\delta^{18}O$ and Ti values from jadeitite zircons are higher than expected for hydrothermal zircons and, although some zircons might be hydrothermal in origin, most zircons are relict igneous crystals inherited from the precursor rocks. The published ages of Burmese jadeitites cannot be interpreted as the ages of jade formation and it can only be assumed that the true age must be younger than *c.* 77 Ma because metasomatic ages must always be younger than the higher pressure–temperature jadeite-forming metamorphic event.

Lake Indawygyi gabbro

Only peridotites and jadeitites are found in the Jade Mines areas around Taw Maw and Hpakant, but, to the south in the Lake Indawgyi area, gabbros are associated with non-jadeitized harzburgites and lherzolites of mantle sequence rocks that are continuous northwards towards the Jade Mines belt. A gabbro outcropping on the shores of Lake Indawgyi at GPS location (25.13.31° N, 96.19.36°E) was sampled for dating (sample MY189). This locality lies NE of the western ophiolite belt, in which the Kaleymyo ophiolite has a U–Pb zircon age of *c.* 127 Ma, and NW of the Tagaung–Myitkyina ophiolite belt that has a U–Pb zircon age of *c.* 173 Ma (Liu *et al.* 2016).

Zircons were separated from MY189 and analysed for both U–Pb and Hf isotopes via laser ablation inductively coupled plasma mass spectrometry (see analytical methods and data tables in the Supplementary data). Thirteen analyses gave a concordia age of 168. 8 ± 0.5 Ma (MSWD 0.39), interpreted as the magmatic age of the rock (Fig. 9). Fifteen Hf isotope analysis range in εHf from 16.6 to 24.7, with a highly juvenile mean εHf of 20.3 ± 2.3 (1σ). These data are on or, in some cases, above the modelled depleted mantle, indicating an extremely short crustal residence time. This Middle Jurassic age is similar to that of the Myitkyina ophiolite, providing strong evidence that the Jade Mines belt was originally part of the Tagaung–Myitkyina suture zone, subsequently offset by Neogene dextral shearing along the Sagaing Fault.

Downloaded from https://www.lyellcollection.org by University of St Andrews Library on Jul 24, 2023

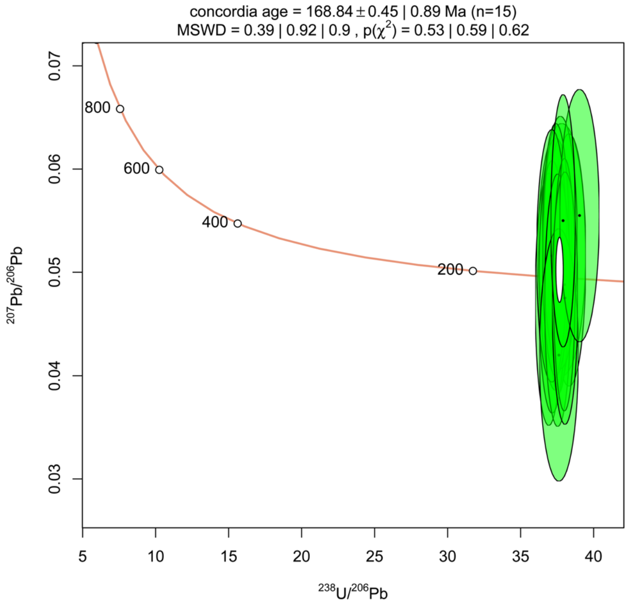

Fig. 9. Tera–Wasserburg U–Pb concordia diagram for sample MY189, a gabbro from the Jade Mines ophiolite, Lake Indawgyi.

Discussion

Comparisons with the Oman (Semail) ophiolite

The Oman ophiolite is by far the largest, best-exposed and most extensively researched ophiolite in the world (Glennie *et al.* 1974; Lippard *et al.* 1986; Searle and Cox 1999, 2002). It consists of *c.* 5–15 km thickness of mantle sequence peridotites, dominantly harzburgites and dunites, overlain by 5–7 km of crustal sequence that includes Moho transition zone layered gabbros and peridotites with late wehrlites, isotropic gabbro lower crust, minor plagiogranites, sheeted dyke complexes and pillow lavas with deep-sea oceanic sediments (radiolarian cherts, Fe- and Mn-rich umbers and oozes). The entire ophiolite was obducted and emplaced onto the continental margin of Arabia during the period *c.* 96–80 Ma (Late Cretaceous). The mantle sequence consists of dominantly harzburgites (olivine + enstatite) and dunites (olivine ± chromite) with rare lherzolites (clinopyroxene-bearing harzburgite) along the base, intruded by pyroxenite (mainly enstatite) dykes (Fig. 6e) and gabbroic sweats (*in situ* mantle melting) with uncommon plagiogranite dykes that are more common in the gabbro sequence. Eclogites and blueschists are present at deep structural levels in Oman, but these are in continental crust units (Permian basalt sills in carbonates) and are not part of the ophiolite thrust sheet (Searle and Cox 1999; Garber *et al.* 2021).

Most of the ophiolite mantle sequence is serpentinized, with the degree of alteration varying with structural depth. At least two main periods of serpentinization are recorded in the Oman ophiolite. The first serpentinization event resulted from fluids fluxing along the subduction interface along the Semail thrust that emplaced the ophiolite. The banded ultramafic unit is composed of totally serpentinized harzburgite and dunite with minor late hornblende and comprises the lowermost 20–100 m of the mantle sequence; this overlies a garnet + diopside amphibolite, which is part of the inverted metamorphic sole (Searle and Malpas 1980, 1982; Ambrose *et al.* 2021). Clinopyroxenite dykes intrude the upper part of the metamorphic sole and the basal harzburgite–dunite mantle sequence (Fig. 6e; Ishimaru *et al.* 2017). These field relationships could be a proxy for the jadeitite dykes intruding serpentinized peridotites in the Hpakant region of the Burmese Jade Mines (Fig. 3).

Grossular-bearing rodingites are associated with this phase of alteration and record Ca-metasomatism of gabbros, whereas silica serpentinites (listwanites and birbirites) record Si-rich fluid infiltration, again along the peridotite–amphibolite contact. Serpentine + quartz assemblages are stable at near-surface temperatures of *c.* 15–50°C (Streit *et al.* 2012). The listwanites in Oman are composed of magnesite + quartz or dolomite + quartz with relict chrome spinel and fuchsite (Falk and Kelemen 2015). Where the silicification is incomplete, reddish brown goethite pseudomorphs of serpentinite and opal, chalcedony or jasper can precipitate (Stanger 1985).

The second serpentinization event was a wholesale serpentinization by large-scale, slightly acidic CO_2-rich meteoritic groundwater, resulting in the leaching of magnesite from dissolved CO_2-rich fluids emanating from the peridotite. The dissolution of serpentinite releases Ni and As from the residual Fe minerals, promoting minor mineralization associated with the serpentinization process. Hyperalkaline groundwater of the calcium hydroxide type with pH values between 11 and 12 (Barnes and O'Neil 1978) forms blue pools throughout the mountains where groundwater flows through serpentinized harzburgite and dunite.

Comparison with the Jijal Complex, Kohistan island arc

The Kohistan island arc consists of a 35–45 km thick section through a Cretaceous island arc sequence in northern Pakistan that was obducted onto the Indian plate margin during the Late Cretaceous prior to the Eocene collision between India and Asia and then subsequently tilted to the north to expose its roots. It represents one of the best cross-sections through a complete oceanic island arc anywhere in the world and is highly valued for exposing deep crustal and upper mantle rocks that are rarely available for study (Jan and Howie 1981; Khan *et al.* 1993; Schaltegger *et al.* 2002).

The Jijal mafic–ultramafic complex forms the deepest exposed levels of the island arc and consists of an upper gabbroic section overlying a thick mantle ultramafic section along the Moho transition zone. Igneous textures in the gabbro are overprinted by granulite facies metamorphism (Garrido *et al.* 2006, 2007; Dhuime *et al.* 2007; George *et al.* 2021). Thermodynamic modelling suggests that the deepest part of the mafic sequence of the Kohistan arc crystallized primary magmatic garnet and clinopyroxene at pressures of 11–14 kbar (George *et al.* 2021). The ultramafic section is composed of a layered dunite, wehrlite and pyroxenite zone, overlain by a websterite–dunite zone and a garnet–hornblendite zone. Dunites are intruded by Cr-rich clinopyroxene veins; these rocks could be analogous to the protoliths of the Burmese jadeitite dykes intruding serpentinized peridotites. The geochemistry indicates that the Jijal mantle rocks (dunite, wehrlite and websterite) are cumulates of boninitic affinity related to the roots of an island arc (Dhuime *et al.* 2007). These are distinctly different from ophiolitic mantle rocks, which are dominated by a cumulate sequence of dunite and orthopyroxenite.

Relationship of jadeitites to calc-alkaline volcanoes

Any tectonic model for the formation of the jadeitites in the Burmese Jade belt must explain why mantle peridotites in this area have been jadeitized, whereas other mantle peridotites nearby have not. One point of interest is the spatial relationship between the jadeitites at Hpakant with a large Pliocene–Quaternary calc-alkaline stratovolcano (Mt Loimuie Bum, 1562 m), immediately NE of Hpakant (Fig. 1). Two other volcanoes, Mt Taung Thonlon (1708 m) and Mt Loimaw (1551 m) occur south of the Jade Mines belt and Lake Indawgyi. These volcanoes lie above the deep Burma seismic zone (Searle *et al.* 2017), an active east-dipping slab

Downloaded from https://www.lyellcollection.org by University of St Andrews Library on Jul 24, 2023

of relict oceanic lithosphere with earthquakes recorded to depths of *c.* 250 km (Stork *et al.* 2008). It is possible that the peridotites of the Jade Mines were originally part of an obducted ophiolite and that fluids emanating from the volcano introduced Na-rich fluids that metasomatically altered the peridotites. Mt Taung Thonlon is, however, located *c.* 55 km SSW of the Jade Mines belt and peridotites around the nearby Indawgyi Lake are normal harzburgites and dunites without jadeite. A relationship between the calc-alkaline volcanoes and the jadeitization of the peridotites therefore seems unlikely.

Relationship of jadeitites to the Sagaing strike-slip fault

One further possibility is that mantle-derived fluids could have been focused along the crustal-scale Sagaing strike-slip fault. The Sagaing Fault runs from the Andaman Sea north to the Jade Mines area (Fig. 1). The fault probably initiated at *c.* 27–20 Ma (Searle *et al.* 2020; Lamont *et al.* 2021) and experienced >400 km of dextral offset (Mitchell *et al.* 2012; Morley 2016; Morley and Arboit 2019). The Jade Mines area lies between the western two strands of the Sagaing Fault (Fig. 2). However, other ophiolitic mantle sequence rocks are abundant in the Tagaung region, where the Myitkyina ophiolites appear to be cut by the Sagaing Fault. These peridotites have extensive Ni laterite deposits and are not jadeitized, questioning this link. Other serpentinite outcrops occur sporadically along the Sagaing Fault, which has also channelled young basaltic magmas to the surface (Bertrand and Rangin 2003). This major plate-bounding, strike-slip fault, initiated after 20–18 Ma, does appear to tap down to the upper mantle, but was not responsible for the formation of jadeitites.

Figure 10a shows a present-day map of the Sagaing Fault, after Mitchell *et al.* (2012) and Sloan *et al.* (2017), showing possible pinning points of the Jade Mines belt, the Myitkyina ophiolite and the Mogok metamorphic belt. Figure 10b is a reconstruction, unwinding the 400 km of dextral slip along the Sagaing Fault. This reconstruction links the western Kaleymyo–Nagaland ophiolites in western Myanmar to the Jade Mines belt and to the similar Jurassic age Myitkyina ophiolite in the Tagaung–Myitkyina belt. This ophiolite belt is interpreted as an extension through SE Asia of the main India–Asia suture along the northern Himalaya (Searle *et al.* 2017; Morley *et al.* 2020).

Harlow *et al.* (2015) suggested that fluid flow is focused by fracture networks associated with large continental strike-slip faults. Although undoubtedly true, this would still not explain high pressures in jadeites or why the exhumed mantle rocks along the Sagaing Fault south of the Jade Mines are normal harzburgites rather than jadeitites.

Model for the formation of the Burmese Jade Mines rocks

Figure 11 shows a model of a typical Pacific-type subduction zone tectonic setting, adapted from Stern *et al.* (2013) and Harlow *et al.* (2015), showing three possible tectonic sites where the Burmese jadeitites could have formed. Site 1 is a typical obducted Tethyan-type ophiolite, represented, for example, by the Oman ophiolite. These Tethyan-type obducted ophiolites do not usually show jadeitites, although ultra-high-pressure eclogites are found at deeper crustal levels in subducted continental crust beneath trailing margins, where they are exposed (e.g. the As Sifah eclogites in Oman). The mantle sequence rocks are typically depleted harzburgites and dunites with chromitites and low-temperature serpentinization. Site 2 is the location of trench mélanges, which typically have a serpentine matrix, contain blocks of high-pressure and ultra-high-pressure rocks, typified by the Syros eclogites in the Aegean and the Franciscan mélanges (Coleman and Wang 1995). The mélanges contain kosmochlore and high-pressure minerals and may contain slices of relatively intact ophiolite within the serpentinite matrix. This is the most likely tectonic setting for the Burmese jadeitites, despite the sparsity of eclogites at Taw Maw and Hpakant. Site 3 is a sub-continental forearc setting where Na-, Al- and Si-rich fluids rise from the subducting slab, resulting in metasomatization of the lithospheric mantle to form jadeitite. A location directly beneath the island arc, such as the Kohistan arc in

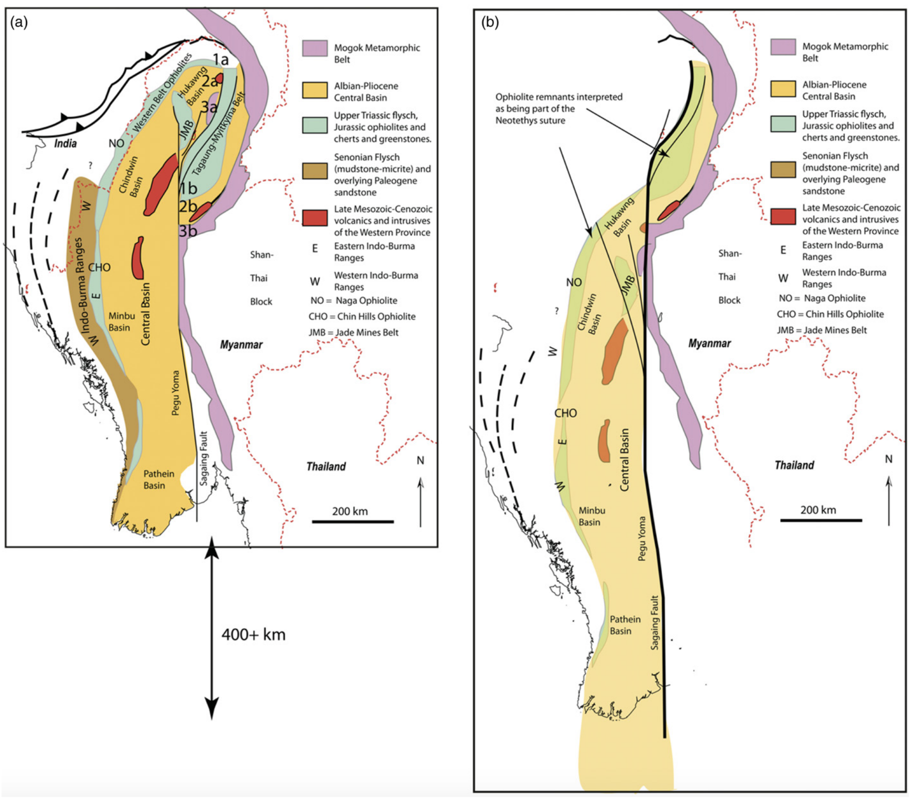

Fig. 10. Simplified geological maps showing proposed dextral offset of *c.* 400 km along the Sagaing Fault since 20–18 Ma. (**a**) Present-day map of the Sagaing Fault showing possible pinning points for restoration. These are numbered and discussed in detail by Sloan et al. (2017). (**b**) Reconstruction of the Sagaing Fault, unwinding the 400 km of dextral slip. This restoration shows that the Tagaung–Myitkyna ophiolite belt, the Jade Mines belt and the Indo-Burma range ophiolite were all part of the main India–Asia suture zone prior to strike-slip faulting. Source: Mitchell et al. (2012) and Sloan et al. (2017).

Downloaded from https://www.lyellcollection.org by University of St Andrews Library on Jul 24, 2023

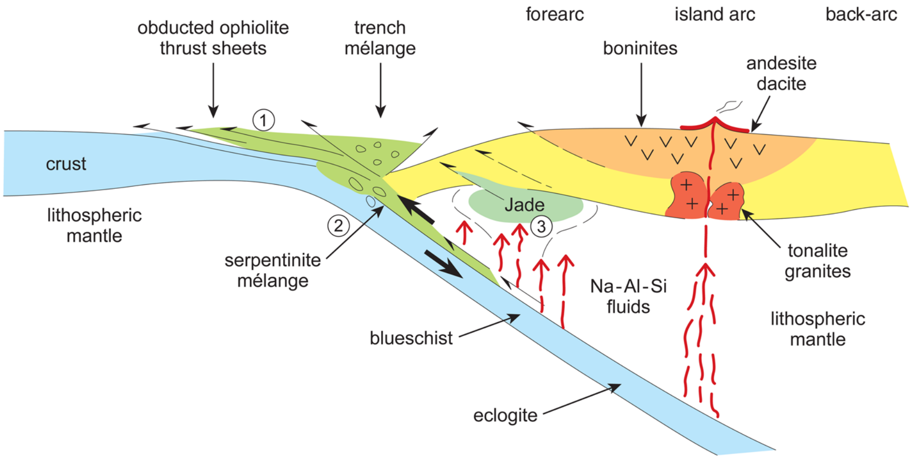

Fig. 11. Model for potential sites of jadeite formation in Myanmar. Eastwards (in present-day coordinates) subduction of Tethyan oceanic crust beneath the Kaleymyo–Nagaland ophiolites and island arc system resulted in the westwards obduction of the ophiolite complexes and the eastwards subduction of serpentinized oceanic mantle and crust. Three possible sites of jadeite formation are: (1) related to the ophiolite complexes; (2) within serpentinized mélanges along the trench; and (3) within the mantle wedge, forming as a result of Na–Al–Si fluids rising from the subduction zone. The sub-continental mantle would be related to the forearc region where boninites are erupted above the subduction zone.

Pakistan, does not generally show jadeitites. A fourth possible location, along the Sagaing transform fault (Nyunt 2009), is not shown on Figure 11 because there are several peridotite locations along the fault south of the Jade Mines where normal harzburgite–lherzolites are present without jade. If there was a causal link between strike-slip faulting and jadeitites, we would expect to find jadeitites along the length of the fault, which is not the case in Myanmar.

We propose a tectonic scenario for the formation of the Burmese Jade Mines rocks that might account for all the geological factors.

(1) *Ophiolite formation stage*. The Jade Belt ophiolite shows a normal mantle sequence of harzburgite–dunite with minor chromitite pods, intruded by orthopyroxenite (enstatite) and clinopyroxenite (diopside) veins and gabbroic dykes. The upper parts of the ophiolite (sheeted dykes, pillow lavas, radiolarian cherts) have not been preserved. Albitite dykes intruding serpentinized peridotites may be metasomatized plagiogranites. Like most ophiolites, these rocks were formed in a supra-subduction zone environment and the fluids driven off the subducting plate rose to cause *in situ* mantle serpentinization. The Taw Maw–Hpakant jadeitites may have formed during this phase by Na–Al–Si fluids driven off a subduction zone and rising to interact with serpentinized peridotites of the mantle sequence (Fig. 11).

(2) *Ophiolite obduction stage*. Obduction of the ophiolite onto the continental crust resulted in the formation of the high-temperature amphibolites and greenschist facies of the metamorphic sole (Searle and Cox 1999, 2002) accreted along the base of the peridotite and fluid-fluxed serpentinization along the thrust contact, resulting in silica-saturated listwanites and Ca-metasomatized rodingites under low-pressure and low-temperature conditions. No eclogite facies metamorphism related to attempted subduction of the continental plate during late-stage ophiolite obduction, as seen in Oman (As Sifah eclogites), is present in outcrop in Myanmar.

(3) *Post-obduction low-temperature–low-pressure serpentinization.* This resulted from regional hydrothermal alteration of olivine by meteoric waters in circulating groundwater.

(4) *Pliocene–Quaternary calc-alkaline dacite–andesite volcanic rocks*. Several major volcanoes were formed above the east-dipping Burma seismic zone, which is a deep zone of earthquakes that penetrates at least 250 km into the mantle. One of the largest of these volcanoes (Mt Loimue Bum, 1562 m) formed immediately NE of the Hpakan jadeitites. Si- and Na-rich fluids released from the volcano's magmatic plumbing system could have reacted with the serpentinized peridotites to form jadeitite (Na-metasomatized pyroxenite), albitite and listwanite (Si-metasomatized peridotite). In this case, the jadeitites are not related to high-pressure metamorphism. Models relating jadeitite formation to either Pliocene–Quaternary volcanoes or Late Miocene to present-day strike-slip shearing along the Sagaing Fault are unlikely given the dated Jurassic gabbro samples from Lake Indawygi.

(5) In situ *weathering of the Hpakant ophiolitic rocks*. As in all ophiolitic mantle rocks, the serpentinization process results in 'chessboard' veining of serpentinites, with extreme alteration around clasts of more resistant peridotite. Serpentine minerals, talc and asbestos are concentrated around more resistant 'boulders' of less serpentinized jadeitites and peridotites (Fig. 6f). Eventually, the process leads to the more resistant cores weathering out and appearing as rounded boulders. The size and scale of some of the Hpakant jadeitic boulders cannot be explained solely by fluvial processes along the relatively minor Uru river valley.

(6) *Limited fluvial transport.* The transport of boulders along the Uru River resulted in sedimentary layering of the jade boulder beds interbanded with clays and mudstones.

Conclusions

Although some exceptional samples of high-quality jade are present in the Jade Mines belt, Myanmar, especially at Taw Maw, many of the ultramafic rocks consist of a variety of altered and highly serpentinized peridotites, including serpentinized lherzolite, harzburgite, dunite and wehrlite, in addition to albitites (meta-plagiogranites) and listwanites (carbonated serpentinite), with a variety of additional trace elements forming the mauve, lilac and dark green varieties. We suggest that all the rocks were originally part of an ophiolitic mantle sequence thrust sheet that was affected by widespread metasomatism. A new U–Pb zircon age from an ophiolitic gabbro from Lake Indawygi gives a Jurassic age of 168. 8 ± 0.5 Ma, similar to the age of the Myitkyina ophiolite (Liu *et al.* 2016), strongly suggesting an ophiolitic origin for the ultramafic and gabbro components. There could possibly have been a major detachment separating the subducted higher pressure mantle component from the crustal gabbroic component. The only true jade is from rocks composed of omphacite, jadeitic pyroxene and kosmochlore, exposed mainly in the Taw Maw area, and many boulders from the Uru conglomerates in Hpakant. Na-, Al- and Si-rich fluids driven off a subducting oceanic plate rose into the mantle wedge to affect the serpentinized peridotites, possibly

Downloaded from https://www.lyellcollection.org by University of St Andrews Library on Jul 24, 2023

associated with some high-pressure metamorphism. All the other occurrences resulted from serpentinization reactions during either initial subduction, or by groundwater alteration, following obduction. No garnet-bearing eclogite nor other high-pressure rocks have been definitively described from the Hpakant jade belt, although Nyunt (2009) has described high-pressure rocks (16–20 kbar) from the Taw Maw region, so it is remotely possible that processes other than subduction could have resulted in the jadeitite formation.

We suggest that the Burmese jadeitites most likely have an ophiolitic origin, either in a deeply subducted mantle wedge beneath a Tethyan-type ophiolite (Fig. 11, Site 2) or in the mantle wedge above a subduction zone (Fig. 11, Site 3). The U–Pb age on the Lake Indawygi gabbro is similar to the age of the Tagaung–Myitkyina ophiolite and we suggest that the two belts were aligned prior to separation along the Sagaing strike-slip fault. Angiboust *et al.* (2021) relate clusters of seismicity in the partly serpentinized mantle wedge in several active subduction zones (Greece, Japan, New Zealand, Chile and Colombia) to the influx of fluids or melts between 30 and 70 km depth. Jadeitites are thought to represent fossilized fluid pathways from the base of the hydrated mantle wedge (Harlow and Sorensen 2005; Harlow *et al.* 2015). The Burmese jadeitites are not related to subducted continental crust, as seen at deep structural levels of the Oman ophiolite, or in the deepest levels of the Himalaya where early ultra-high-pressure eclogite facies metamorphism has been overprinted by later regional granulite–amphibolite facies metamorphism (Liou *et al.* 2004; Searle 2015).

The close association of the Jade belt at Hpakant with the large andesite–dacite volcanoes, Mt Loimue and Taung Thonlong, could suggest a causal link, with fluids driven off the subducting slab beneath the volcano altering the overlying peridotites, although this would not explain the high-pressure conditions nor the U–Pb age of the associated gabbro. None of the Burmese or Nagaland–Manipur ophiolites in the Indo-Burma Ranges, nor those along the Tagaung–Myitkyina belt, has exposed jadeitites. All the mantle sequence rocks here are normal serpentinized harzburgite–dunites. North and south of Taw Maw and Hpakant, similar peridotites remain non-jadeitized and instead show normal harzburgite–dunites affected by serpentinization, as seen in most other ophiolites. Jade and serpentinized peridotite boulders are found in the famous boulder beds of the Uru River and have always been attributed to fluvial processes along the river. However, normal chessboard serpentinization and weathering processes also form boulders when the softer talc–serpentine weathers out the rounded boulders. Only the final deposition along the Uru River can be attributed to fluvial processes.

Scientific editing by Wenjiao Xiao

Acknowledgements We thank Than Than Nu and Ney Lin of Mandalay University for discussions, Htun Lyn Shein (Myanmar Precious Resources Group) for help in obtaining the samples and Doug Kirwin for his photographs of the Taw Maw jadeitite. We thank Chris Morley and an anonymous reviewer for helpful comments.

Author contributions **MPS**: conceptualization (lead), funding acquisition (lead), investigation (equal), project administration (equal), writing – original draft (lead), writing – review and editing (lead); **RMP**: formal analysis (equal), investigation (equal), writing – review and editing (supporting); **NJG**: conceptualization (equal), investigation (equal); **KH**: conceptualization (equal), investigation (equal); **JW**: data curation (supporting).

Funding MPS and NJG thank the Oxford–Burma Aung San Suu Kyi Trust and the Fell Fund for funding the fieldwork in Myanmar.

Competing interests The authors declare that they have no known competing financial interests or personal relationships that could have appeared to influence the work reported in this paper.

Data availability All the data are archived at https://ora.ox.ac.uk

References

Acharyya, S.K. 2007. Collisional emplacement history of the Naga–Andaman ophiolites and the position of the eastern Indian suture. *Journal of Asian Earth Sciences*, **29**, 29–242, https://doi.org/10.1016/j.jseaes.2006.03.003

Acharyya, S.K. 2010. Tectonic evolution of the Indo-Burma ranges with special reference of Naga–Manipur Hills. *Geological Survey of India, Memoirs*, **75**, 25–43.

Ambrose, T.K., Waters, D.J., Searle, M.P., Gopon, P. and Forshaw, J.B. 2021. Burial, accretion and exhumation of the metamorphic sole of the Oman–UAE ophiolite. *Tectonics*, **40**, e2020TC006392, https://doi.org/10.1029/2020TC006392

Angiboust, S., Montecinos, J.M., Cambeses, A., Raimondo, T., Deldicque, D. and Garcia-Casco, A. 2021. Jolts in the jade factory: a route for subduction fluids and their implications for mantle wedge seismicity. *Earth Science Reviews*, **220**, 103720, https://doi.org/10.1016/j.earscirev.2021.103720

Ao, A. and Bhowmik, S.K. 2014. Cold subduction of the Neotethys: the metamorphic record from finely-banded lawsonite and epidote blueschists and associated metabasalts of the Nagaland Ophiolite Complex, India. *Journal of Metamorphic Geology*, **32**, 829–860, https://doi.org/10.1111/jmg.12096

Barnes, I. and O'Neil, J.R. 1978. Present day serpentinisation in New Caledonia, Oman and Yugoslavia. *Geochimica et Cosmochimica Acta*, **42**, 144–145, https://doi.org/10.1016/0016-7037(78)90225-9

Bauer, M. 1895. On the jadeite and other rocks from Tawmaw in Upper Burma. *Records of the Geological Survey of India*, **28**, 91–105.

Bender, F. 1983. *The Geology of Burma*. Gebrüder Borntraeger, Berlin.

Bertrand, G. and Rangin, C. 2003. Tectonics of the western margin of the Shan Plateau (central Myanmar): implications for the India–Indochina oblique convergence since the Oligocene. *Journal of Asian Earth Sciences*, **21**, 1139–1157, https://doi.org/10.1016/S1367-9120(02)00183-9

Bleeck, A.W.G. 1908. Jadeite in the Kachin Hills, Upper Burma. *Records of the Geological Survey of India*, **36**, 254–285.

Buckman, S. and Ashley, P.M. 2010. Silica–carbonate (listwanites) related gold mineralisation associated with epithermal alteration of serpentinite bodies. *In*: Buckman, S. and Blevin, P.L. (eds) *New England Orogen 2010: Proceedings of a Conference Held at the University of New England, Armidale, New South Wales, Australia, November 2010*. 94–105.

Chen, Y., Yang, J., Xu, Z., Tian, Y. and Lai, S. 2018. Diamonds and other unusual minerals from peridotites of the Myitkyina ophiolite, Myanmar. *Journal of Asian Earth Sciences*, **164**, 179–193, https://doi.org/10.1016/j.jseaes.2018.06.018

Chhibber, H.L. 1934*a*. *The Mineral Resources of Burma*. MacMillan, London.

Chhibber, H.L. 1934*b*. *The Geology of Burma*. MacMillan, London.

Coleman, R.G. and Wang, X. 1995. *Ultrahigh Pressure Metamorphism*. Cambridge University Press, Cambridge.

Compagnoni, R., Rolfo, F. and Catelli, D. 2012. Jadeite from the Monviso meta-ophiolite, Western Alps: occurrence and genesis. *European Journal of Mineralogy*, **24**, 333–343, https://doi.org/10.1127/0935-1221/2011/0023-2164

De Capitani, C. and Petrakakis, K. 2010. The computation of equilibrium assemblage diagrams with Theriak/Domino software. *American Mineralogist*, **95**, 1006–1016, https://doi.org/10.2138/am.2010.3354

Dhuime, B., Bosch, D., Bodinier, J.-L., Garrido, C.J., Bruguier, O., Hussain, S. and Dawood, H. 2007. Multistage evolution of the Jijal ultramafic–mafic complex (Kohistan, N. Pakistan): implications for building the roots of island arcs. *Earth and Planetary Science Letters*, **261**, 179–200, https://doi.org/10.1016/j.epsl.2007.06.026

Falk, E.S. and Kelemen, P. 2015. Geochemistry and petrology of listvenite in the Semail ophiolite, Sultanate of Oman: complete carbonation of peridotite during ophiolite emplacement. *Geochimica et Cosmochimica Acta*, **160**, 70–90, https://doi.org/10.1016/j.gca.2015.03.014

Fu, B., Valley, J.W. *et al.* 2010. Multiple origins of zircons in jadeitite. *Contributions to Mineralogy and Petrology*, **159**, 769–780, https://doi.org/10.1007/s00410-009-0453-y

Garber, J.M., Rioux, M. *et al.* 2021. Dating continental subduction beneath the Samail Ophiolite: garnet, zircon, and rutile petrochronology of the As Sifah eclogites, NE Oman. *Journal of Geophysical Research: Solid Earth*, **126**, e2021JB022715, https://doi.org/10.1029/2021JB022715

Gardiner, N.J., Searle, M.P., Morley, C.K., Whitehouse, M.J., Spencer, C.J. and Robb, L.J. 2016. The closure of Palaeo-Tethys in eastern Myanmar and northern Thailand: new insights from zircon U–Pb and Hf isotope data. *Gondwana Research*, **39**, 401–422, https://doi.org/10.1016/j.gr.2015.03.001

Gardiner, N.J., Searle, M.P. *et al.* 2018. The crustal architecture of Myanmar imaged through zircon, U–Pb, Lu–Hf and O isotopes: tectonic and metallogenic implications. *Gondwana Research*, **62**, 27–60, https://doi.org/10.1016/j.gr.2018.02.008

Garrido, C.J., Bodinier, J.-L. *et al.* 2006. Petrogenesis of mafic garnet granulite in lower crust of the Kohistan Paleo-arc complex (northern Pakistan): implications for intra-crustal differentiation of island arcs and generation of continental crust. *Journal of Petrology*, **47**, 1873–1914, https://doi.org/10.1093/petrology/egl030

Downloaded from https://www.lyellcollection.org by University of St Andrews Library on Jul 24, 2023

Garrido, C.J., Bodinier, J.-L. *et al.* 2007. Origin of the island arc Moho transition zone via melt–rock reaction and its implications for intracrustal differentiation of island arc: evidence from the Jijal complex (Kohistan complex, northern Pakistan). *Geology*, **35**, 683–686, https://doi.org/10.1130/G23675A.1

George, F.R., Waters, D.J., Gough, S.J., Searle, M.P. and Forshaw, J.B. 2021. Phase equilibria and microstructural constraints on the high-T building of the Kohistan island arc: the Jijal garnet granulites, northern Pakistan. *Journal of Metamorphic Geology*, **40**, 145–174, https://doi.org/10.1111/jmg.12622

Glennie, K.W., Boeuf, M.G., Hughes-Clarke, M.H.W., Moody-Stuart, M., Pilaar, W.F. and Reinhardt, B.M. 1974. *Geology of the Oman Mountains*. Verhandelingen Koninklijk Nederlands Geologisch Mijnbouwkundidg Genootschap, The Hague.

Global Witness 2015. *Jade: Myanmar's 'Big State Secret'*. Global Witness, London.

Grant, J.A. 2005. Isocon analysis: a brief review of the method and applications. *Physics and Chemistry of the Earth, Parts A/B/C*, **30**, 997–1004, https://doi.org/10.1016/j.pce.2004.11.003

Gübelin, E. 1965. Maw-sit-sit – a new decorative gemstone from Burma. *Journal of Gemmology*, **9**, 329–344, https://doi.org/10.15506/JoG.1965.9.10.329

Hansen, L.D., Dipple, G.M., Kellett, D.A. and Gordon, T.M. 2005. Carbonate altered serpentinite (listwanite) at Atlin, British Columbia: a geological analogue to carbon dioxide sequestration. *Canadian Mineralogist*, **43**, 225–239, https://doi.org/10.2113/gscanmin.43.1.225

Harlow, G.E. 1994. Jadeitites, albitites and related rocks from the Motagua Fault Zone, Guatemala. *Journal of Metamorphic Geology*, **12**, 49–68, https://doi.org/10.1111/j.1525-1314.1994.tb00003.x

Harlow, G.E. and Sorensen, S.S. 2001. Jade: occurrence and metasomatic origin. *Australian Gemmologist*, **21**, 7–10.

Harlow, G.E. and Sorensen, S.S. 2005. Jade (nephrite and jadeitite) and serpentinite: metasomatic connections. *International Geology Review*, **47**, 113–146, https://doi.org/10.2747/0020-6814.47.2.113

Harlow, G.E., Tsujimori, T. and Sorensen, S.S. 2015. Jadeitites and plate tectonics. *Annual Reviews of Earth and Planetary Sciences*, **43**, 105–138, https://doi.org/10.1146/annurev-earth-060614-105215

Holland, T.J.B. and Powell, R. 2011. An improved and extended internally consistent thermodynamic dataset for phases of petrological interest, involving a new equation of state for solids. *Journal of Metamorphic Geology*, **29**, 333–383, https://doi.org/10.1111/j.1525-1314.2010.00923.x

Hughes, R.W., Galibert, O. *et al.* 2000. Burmese jade: the inscrutable gem. *Gems and Gemmology*, **36**, 2–26, https://doi.org/10.5741/GEMS.36.1.2

Hutchison, C.S. 1975. Ophiolite in SE Asia. *Geological Society of America Bulletin*, **86**, 797–806, https://doi.org/10.1130/0016-7606(1975)86<797:OISA>2.0.CO;2

Ishimaru, S., Arai, S. and Tamura, A. 2017. Clinopyroxenite dykes within a banded unit in the basal mantle section of the northern part of the Oman ophiolite: a record of latest deep-seated magmatism. *Lithos*, **292–293**, 334–347, https://doi.org/10.1016/j.lithos.2017.09.022

Jan, M.Q. and Howie, R.A. 1981. The mineralogy and geochemistry of metamorphosed basic and ultrabasic rocks of the Jijal Complex, Kohistan, NW Pakistan. *Journal of Petrology*, **22**, 85–126, https://doi.org/10.1093/petrology/22.1.85

Jennings, E.S. and Holland, T.J. 2015. A simple thermodynamic model for melting of peridotite in the system NCFMASOCr. *Journal of Petrology*, **56**, 869–892, https://doi.org/10.1093/petrology/egv020

Kelemen, P. and Matter, J.M. 2008. In situ carbonation of peridotite for CO_2 storage. *Proceedings of the National Academy of Sciencs of the USA*, **105**, 17295–17300, https://doi.org/10.1073/pnas.0805794105

Khan, M.A., Jan, M.Q. and Weaver, B.L. 1993. Evolution of the lower arc crust in Kohistan, N Pakistan: temporal arc magmatism through early, mature and intra-arc rift stages. *Geological Society, London, Special Publications*, **74**, 123–138, https://doi.org/10.1144/GSL.SP.1993.074.01.10

Lamont, T.N., Searle, M.P. *et al.* 2021. Late Eocene–Oligocene granulite facies garnet–sillimanite migmatites from the Mogok metamorphic belt, Myanmar, and implications for timing of slip along the Sagaing Fault. *Lithos*, **386–387**, 106027, https://doi.org/10.1016/j.lithos.2021.106027

Liou, J.G., Tsujimori, T., Zhang, R.Y., Katayama, I. and Maruyama, S. 2004. Global UHP metamorphism and continental subduction/collision: the Himalayan model. *International Geological Review*, **46**, 1–27, https://doi.org/10.2747/0020-6814.46.1.1

Lippard, S.J., Shelton, A.W. and Gass, I.G. (eds) 1986. *The Ophiolite of Northern Oman*. Geological Society, London, Memoirs, **11**.

Liu, C.-Z., Chung, S.-L., Wu, F.W., Zhang, C., Xu, Y., Wang, J.-G. and Chen, Y. 2016. Tethyan suturing in Southeast Asia: zircon U–Pb and Hf–O isotopic constraints from Myanmar ophiolites. *Geology*, **44**, 311–314, https://doi.org/10.1130/G37342.1

Manning, C.E. 2004. The chemistry of subduction zone fluids. *Earth and Planetary Science Letters*, **223**, 1–16, https://doi.org/10.1016/j.epsl.2004.04.030

Maung, H. 1987. Transcurrent movements in the Burma–Andaman Sea region. *Geology*, **15**, 911–912, https://doi.org/10.1130/0091-7613(1987)15<911:TMITBS>2.0.CO;2

Maurin, T., Masson, F., Rangin, C., Than Min, U. and Collard, P. 2010. First global positioning system results in northern Myanmar: constant and localised slip along the Sagaing Fault, Geology, **38**, 591–594, https://doi.org/10.1130/G30872.1

Mitchell, A.H.G. 1993. Cretaceous–Cenozoic tectonic events in the western Myanmar (Burma)-Assam region. *Journal of the Geological Society, London*, **150**, 1089–1102. https://doi.org/10.1144/gsjgs.150.6.1089

Mitchell, A.H.G. 2018. *Geological Belts, Plate Boundaries and Mineral Resources in Myanmar*. Elsevier.

Mitchell, A.H.G., Chung, S.-L., Oo, T., Lin, T.H. and Hung, C.H. 2012. Zircon U–Pb ages in Myanmar: magmatic–metamorphic events and closure of a Neo-Tethys ocean? *Journal of Asian Earth Sciences*, **56**, 1–23, https://doi.org/10.1016/j.jseaes.2012.04.019

Mitchell, A.H.G., Myint Thein Htay and Kyaw Min Htun 2021. Middle Jurassic arc reversal, Victoria-Katha Block and Sibumasu terrane collision, jadeite formation and Wester Tin Belt generation, Myanmar. *Geological Magazine*, https://doi.org/10.1017/S0016756821000066

Moody, J.B. 1976. Serpentinization: a review. *Lithos*, **9**, 125–138, https://doi.org/10.1016/0024-4937(76)90030-X

Morley, C.K. 2016. Syn-kinematic sedimentation at a releasing splay in the north Minwun Ranges, Sagaing Fault zone, Myanmar: significance for fault timing and displacement. *Basin Research*, **29**, 684–700, https://doi.org/10.1111/bre.12201

Morley, C.K. and Arboit, F. 2019. Dating the onset of motion on the Sagaing fault: evidence from detrital zircon and titanite U–Pb geochronology from the North Minwun Basin, Myanmar. *Geology*, **47**, 581–585, https://doi.org/10.1130/G46321.1

Morley, C.K. and Searle, M.P. 2017. Regional tectonics, structure and evolution of the Andaman–Nicobar islands from ophiolite formation and obduction to collision and back-arc spreading. *Geological Society, London, Memoirs*, **47**, 51–74, https://doi.org/10.1144/M47.5

Morley, C.K., Naing, T., Searle, M.P. and Robinson, S.A. 2020. Structural and tectonic development of the Indo-Burman Ranges. *Earth Science Reviews*, **200**, 102992, https://doi.org/10.1016/j.earscirev.2019.102992

Morley, C.K., Chantraprasert, S., Kongchum, J. and Chenoll, K. 2021. The West Burma terrane, a review of recent paleo-latitude data, its geological implications and constraints. *Earth Science Reviews*, **230**, 103722, https://doi.org/10.1016/j.earscirev.2021.103722

Myanmar Geosciences Society 2012. *Geological Map of Myanmar*. Myanmar Geosciences Society, Yangon.

Ng, Y.-N., Shi, G.-H. and Santosh, M. 2016. Titanite-bearing omphacitite from the Jade Tract, Myanmar: interpretation from mineral and trace element compositions. *Journal of Asian Earth Sciences*, **117**, 1–12, https://doi.org/10.1016/j.jseaes.2015.12.011

Noetling, F. 1893. Note on the occurrence of jadeite in Upper Burma. *Records of the Geological Survey of India*, **26**, 26–31.

Nyunt, T.T. 2009. *Petrological and Geochemical Contribution to the Origin of Jadeitite and Associated Rocks of the Tawmaw Area, Kachin State, Myanmar*. PhD thesis, University of Stuttgart.

Nyunt, T.T., Massonne, H.-J. and Sun, T.T. 2017. Jadeitite and other high-pressure metamorphic rocks from the Jade Mines Belt, Tawmaw area, Kachin State, northern Mynamar. *Geological Society, London, Memoirs*, **48**, 297–317, https://doi.org/10.1144/M48.13

Okay, A.I. 1997. Jadeite–K-feldspar rocks and jadeitites from northwest Turkey. *Mineralogical Magazine*, **61**, 835–843, https://doi.org/10.1180/minmag.1997.061.409.06

Palin, R.M., Weller, O.M., Waters, D.J. and Dyck, B. 2016. Quantifying geological uncertainty in metamorphic phase equilibria modelling; a Monte Carlo assessment and implications for tectonic interpretations. *Geoscience Frontiers*, **7**, 591–607, https://doi.org/10.1016/j.gsf.2015.08.005

Ridd, M.F., Crow, M.J. and Morley, C.K. 2019. The role of strike-slip faulting in the history of the Hukawng Block and the Jade Mines Uplift, Myanmar. *Proceedings of the Geologists' Association*, **130**, 126–141, https://doi.org/10.1016/j.pgeola.2019.01.002

Ringwood, A.E. 1975. *Composition and Petrology of the Earth's Mantle*. MacGraw-Hill, Maidenhead.

Robinson, P.T., Trumbull, R.B. *et al.* 2015. The origin and significance of crustal minerals in ophiolitic chromitites and peridotites. *Gondwana Research*, **27**, 486–506, https://doi.org/10.1016/j.gr.2014.06.003

Schaltegger, U., Zeilinger, G., Frank, M., and Burg, J-P. 2002. Multiple mantle sources during island arc magmatism: U–Pb and Hf isotopic evidence from the Kohistan arc, Pakistan. *Terra Nova*, **14**, 461–468, https://doi.org/10.1046/j.1365-3121.2002.00432.x

Searle, M.P. 2015. Mountain building, tectonic evolution, rheology, and crustal flow in the Himalaya, Karakoram, and Tibet. *In:* Schubert, G. (ed.) *Treatise on Geophysics*. Vol. 6, 2nd edn., Elsevier, 469–511, https://doi.org/10.1016/B978-0-444-53802-4.00121-4

Searle, M.P. and Cox, J.S. 1999. Tectonic setting, origin and obduction of the Oman ophiolite. *GSA Bulletin*, **111**, 104–122, https://doi.org/10.1130/0016-7606(1999)111<0104:TSOAOO>2.3.CO;2

Searle, M.P. and Cox, J.S. 2002. Subduction zone metamorphism during formation and emplacement of the Semail Ophiolite in the Oman Mountains. *Geological Magazine*, **139**, 241–255, https://doi.org/10.1017/S0016756 802006532

Searle, M.P. and Malpas, J. 1980. The structure and metamorphism of rocks beneath the Semail Ophiolite of Oman and their significance in ophiolite obduction. *Transactions of the Royal Society of Edinburgh, Earth Sciences*, **71**, 247–262, https://doi.org/10.1017/S0263593300013614

Downloaded from https://www.lyellcollection.org by University of St Andrews Library on Jul 24, 2023

Searle, M.P. and Malpas, J. 1982. Petrochemistry and origin of sub-ophiolite metamorphic and related rocks in the Oman Mountains. *Journal of Geological Society, London*, **139**, 235–248, https://doi.org/10.1144/gsjgs.139.3.0235

Searle, M.P. and Morley, C.K. 2011. Tectonic and thermal evolution of Thailand in the regional context of SE Asia. *In*: Ridd, M.F., Barber, A.J. and Crow, M.J. (eds) *The Geology of Thailand*. Geological Society, London, 539–571, https://doi.org/10.1144/GOTH.20

Searle, M.P., Noble, S.R., Cottle, J.M., Waters, D.J., Mitchell, A.H.G., Hlaing, T. and Hortswood, M.S.A. 2007. Tectonic evolution of the Mogok metamorphic belt, Burma (Myanmar) constrained by U–Th–Pb dating of metamorphic and magmatic rocks. *Tectonics*, **26**, https://doi.org/10.1029/2006TC002083

Searle, M.P., Morley, C.K., Waters, D.J., Gardiner, N.J., Htun, K., Nu, T.T. and Robb, L.J. 2017. Tectonic and metamorphic evolution of the Mogok Metamorphic and Jade Mines belts and ophiolitic terranes of Burma (Myanmar). *Geological Society, London, Memoirs*, **48**, 263–295, https://doi.org/10.1144/M48.12

Searle, M.P., Garber, J.M., Hacker, B.R., Htun, K., Gardiner, N.J., Waters, D.J. and Robb, L.J. 2020. Timing of syenite–charnokite magmatism and ruby and sapphire metamorphism in the Mogok Valley region, Myanmar. *Tectonics*, **39**, https://doi.org/10.1029/2019TC005998

Shi, G., Cui, W.Y., Liu, D. and Yu, H.X. 2001. The petrology of jadeite-bearing serpentinised peridotite and its country rocks from Northwestern Myanmar. *Acta Petrologica Sinica*, **17**, 483–490.

Shi, G., Cui, W. *et al.* 2008. Ion microprobe zircon U–Pb age and geochemistry of the Myanmar jadeite. *Journal of the Geological Society, London*, **165**, 221–234, https://doi.org/10.1144/0016-76492006-119

Shi, G., Harlow, G.E. *et al.* 2012. Mineralogy of jadeitite and related rocks from Myanmar: a review with new data. *European Journal of Mineralogy*, **24**, 345–370, https://doi.org/10.1127/0935-1221/2012/0024-2190

Shi, G., Lei, W. *et al.* 2014. Superimposed tectono-metamorphic episodes of Jurassic and Eocene age in the jadeite uplift, Myanmar as revealed by $^{40}Ar/^{39}Ar$ dating. *Gondwana Research*, **26**, 464–474, https://doi.org/10.1016/j.gr.2013.08.007

Singh, A.K., Chung, S.-L., Bikramaditya, R.K. and Lee, H.Y. 2016. New U–Pb zircon ages of plagiogranites from the Nagaland–Manipur orogenic belt, NE India. *Journal of the Geological Society, London*, **174**, 170–179, https://doi.org/10.1144/jgs2016-048

Sloan, R.A., Elliott, J.R., Searle, M.P. and Morley, C.K. 2017. Active tectonics of Myanmar and the Andaman Sea. *Geological Society, London, Memoirs*, **48**, 19–52, https://doi.org/10.1144/M48.2

Sorensen, S.S. and Harlow, G.E. 1999. The geochemical evolution of jadeite-depositing fluids. *GSA Abstracts with Programs*, **31**, A-101.

Stanger, G. 1985. Silicified serpentinite in the Semail nappe of Oman. *Lithos*, **18**, 13–22, https://doi.org/10.1016/0024-4937(85)90003-9

Stern, R.J., Tsujimori, T., Harlow, G. and Groat, L.A. 2013. Plate tectonic gemstones. *Geology*, **41**, 723–726, https://doi.org/10.1130/G34204.1

Stork, A., Selby, N.D., Heyburn, R. and Searle, M.P. 2008. Accurate relative earthquake hypocenters reveal structure of the Burma Seismic Zone. *Bulletin of the Seismological Society of America*, **98**, 2815–2827, https://doi.org/10.1785/0120080088

Streit, E., Kelemen, P. and Eiler, J. 2012. Coexisting serpentine and quartz from carbonate-bearing serpentinized peridotite in the Semail Ophiolite, Oman. *Contributions to Mineralogy and Petrology*, **164**, 821–837, https://doi.org/10.1007/s00410-012-0775-z

Syracuse, E.M., van Keken, P.E. and Abers, G.A. 2010. The global range of subduction zone thermal models. *Physics of the Earth and Planetary Interiors*, **183**, 73–90, https://doi.org/10.1016/j.pepi.2010.02.004

Tsujimori, T. and Harlow, G.E. 2012. Petrogenetic relationships between jadeitite and associated high-pressure and low-temperature metamorphic rocks in worldwide jadeitite localities: a review. *European Journal of Mineralogy*, **24**, 371–390, https://doi.org/10.1127/0935-1221/2012/0024-2193

Vigny, C., Socquet, A. *et al.* 2003. Present day crustal deformation around the Sagaing Fault, Myanmar. *Journal of Geophysical Research*, **108**, 2533, https://doi.org10.1029/2002JB001999

Whitney, D.L. and Evans, B.W. 2010. Abbreviations for names of rock-forming minerals. *American Mineralogist*, **95**, 185–187, https://doi.org/10.2138/am.2010.3371

Wulff-Pedersen, E., Neumann, E.R. and Jensen, B.Á. 1996. The upper mantle under La Palma, Canary Islands: formation of Si−K−Na-rich melt and its importance as a metasomatic agent. *Contributions to Mineralogy and Petrology*, **125**, 113–139, https://doi.org/10.1007/s004100050210

Yui, T.-F., Fukoyama, M., Iizuka, Y., Wu, C.-M., Wu, T.-W., Liou, J.G. and Grove, M. 2013. Is Myanmar jadeite of Jurassic age? A result from incompletely recrystallized inherited zircon. *Lithos*, **160–161**, 268–282, https://doi.org/10.1016/j.lithos.2012.12.011

Xu Yang, Liu, C.-Z., Chen, Y., Wang, J.-G. and Kyaing Sein, 2017. Petrogenesis and tectonic implications of gabbro and plagiogranite intrusions in mantle peridotites of the Myitkyina ophiolite, Myanmar. *Lithos*, **284**, 180–193, https://doi.org/10.1016/j.lithos.2017.04.014

Zhou, M.-F., Robinson, P.T., Ben-Xun, S., Gao, J.-F., Li, J.-W. and Yang, J.-S. 2014. Compositions of chromite, associated minerals and parental magmas of podiform chromite deposits: the role of slab contamination of asthenospheric melts in supra-subduction zone environments. *Gondwana Research*, **26**, 262–283, https://doi.org/10.1016/j.gr.2013.12.011